Safety21
INNOVATING FOR SAFETY

US DOT National
University Transportation Center for Safety

Carnegie Mellon University

Penn University of Pennsylvania · The Ohio State University · CCAC Community College of Allegheny County · Community College of Philadelphia · The University of Texas Rio Grande Valley · Morgan State University

SALUSLux: Automation for Safer Pedestrian Street Lighting at Intersections

PI: Katherine A. Flanigan

ORCID: 0000-0002-2454-5713

Final Report – July 31, 2025

DISCLAIMER

The contents of this report reflect the views of the authors, who are responsible for the facts and the accuracy of the information presented herein. This document is disseminated in the interest of information exchange. The report is funded, partially or entirely, under [grant number 69A3552344811 / 69A3552348316] from the U.S. Department of Transportation's University Transportation Centers Program. The U.S. Government assumes no liability for the contents or use thereof.

Technical Report Documentation Page

1. Report No. 496	**2. Government Accession No.**	**3. Recipient's Catalog No.**
4. Title and Subtitle SALUSLux: Automation for Safer Pedestrian Street Lighting at Intersections		**5. Report Date** July 31, 2025
		6. Performing Organization Code Enter any/all unique numbers assigned to the performing organization, if applicable.
7. Author(s) Katherine A. Flanigan, Ph.D. https://orcid.org/0000-0002-2454-5713 Korawich Kavee https://orcid.org/0000-0003-1101-0995 Stephen L. Quick https://orcid.org/0000-0003-1625-485X		**8. Performing Organization Report No.** Enter any/all unique alphanumeric report numbers assigned by the performing organization, if applicable.
9. Performing Organization Name and Address Carnegie Mellon University 5000 Forbes Avenue, Pittsburgh, PA 15213		**10. Work Unit No.**
		11. Contract or Grant No. Federal Grant # 69A3552344811 / 69A3552348316
12. Sponsoring Agency Name and Address Enter name and address of the organization(s) financially responsible for the work. After each agency name, enter funding type (e.g. SPR). Example: Missouri Department of Transportation (SPR)		**13. Type of Report and Period Covered** Final Report (July 1, 2024 – June 30, 2025)
		14. Sponsoring Agency Code USDOT
15. Supplementary Notes Conducted in cooperation with the U.S. Department of Transportation, Federal Highway Administration. The developed SALUSLux toolkit is available open-source at: https://github.com/CMU-SALUS-Lab/saluslux.		

16. Abstract

This study addresses the trade-off between pedestrian visibility, pedestrian safety, and light pollution in nighttime intersection lighting design by analyzing how combinations of light source characteristics (e.g., correlated color temperature, distribution type) and streetlight geometry (e.g., pole height, orientation, offset) affect safety and environmental outcomes. We developed SALUSLux, an open-source, Python-based simulation toolset that evaluates realistic lighting conditions using standardized photometric data, simulating 2,304 intersection scenarios across various spatial configurations and light sources. Results reveal that interaction effects between geometry and luminaire properties are critical, with optimized designs—particularly using lower-correlated color temperature sources and a 45° modified turbine configuration—achieving superior visibility and reduced light pollution. Some designs simultaneously maximized safety and environmental performance, challenging assumptions that brighter or high-correlated color temperature lighting is necessary. This work highlights the potential of tools like SALUSLux to enable data-driven, sustainable streetlighting solutions.

17. Key Words	**18. Distribution Statement**
Pedestrian visibility, pedestrian safety, light pollution, photometric analysis, open-source simulation tools, lighting configuration and optimization.	No restrictions. This document is available through the National Technical Information Service, Springfield, VA 22161. Enter any other agency mandated distribution statements. Remove NTIS statement if it does not apply.

19. Security Classif. (of this report)	**20. Security Classif. (of this page)**	**21. No. of Pages**	**22. Price**
Enter security classification of this report (e.g. Unclassified). Reports carrying a security classification will require additional marking giving security and downgrading information as specified by the sponsoring agency.	Enter the security classification of the form (e.g. Unclassified). When at all possible, this form should remain unclassified. If a classification is required, identify the classified items on the page by an appropriate symbol as per instruction from the sponsoring agency.	Enter the total number of pages in the report, including both sides of all pages and the front and back covers.	Refers to the price of the report. Leave blank unless applicable.

Form DOT F 1700.7 (8-72) Reproduction of completed page authorized

Executive Summary

Pedestrian visibility at intersections is a critical concern for nighttime traffic safety, yet lighting designs often trade off safety benefits with increased light pollution. This study investigates how combinations of light source characteristics (e.g., correlated color temperature (CCT), distribution type) and streetlight geometry (e.g., pole height, orientation, offset) impact both pedestrian visibility and environmental acceptability.

To answer these questions, we developed SALUSLux, an open-source, Python-based simulation software capable of analyzing realistic lighting conditions from standardized photometric data (IES files). We simulated 2,304 intersection lighting scenarios varying across light source types and spatial configurations.

Our findings show that:

- Interaction effects matter: Neither intersection streetlighting geometry nor luminaire properties should be optimized in isolation.
- Lower-CCT sources (e.g., 2,700K light-emitting diodes), often favored for environmental reasons, can meet or exceed performance thresholds when paired with optimized geometries.
- The 45° modified turbine configuration consistently outperformed the traditional 90° setup in crosswalk visibility metrics such as vertical and horizontal illuminance of previous studies using semi-cylindrical illuminance metrics to achieve and exceed equivalent vertical and horizontal illuminance regulatory requirements.
- Importantly, some lighting designs achieved perfect scores for both pedestrian safety and light pollution control, challenging the assumption that visibility requires high-CCT or overly bright lighting.

This work demonstrates that intersection lighting design can be smarter, not just brighter, and that future tools like SALUSLux, a comprehensive app that analyzes complete intersections, can support nuanced, data-driven design for safer and more sustainable urban environments.

Table of Contents

1. Introduction

Pedestrian safety remains a persistent and urgent challenge in transportation systems, especially for vulnerable road users navigating urban environments. Research consistently shows that pedestrian fatalities are significantly more likely to occur in dark conditions. One study found that crashes are 6.5 to 7 times more likely in darkness (Younes et al., 2023), while another reported that vulnerable road users are three to nearly seven times more likely to be involved in a crash at night compared to the day (Sullivan & Flannagan, 1999). In fact, the night-to-day crash ratio is widely recognized as one of the most important indicators used to assess pedestrian lighting needs (Vanasse Hangen Brustlin, Inc. et al., 2022).

Lighting is one of the most powerful interventions for improving nighttime safety. A meta-analysis found that public lighting is associated with a 65% reduction in nighttime fatal accidents, a 30% reduction in nighttime injury accidents, and a 15% reduction in nighttime property-damage-only accidents (Elvik, 1995). Another meta-analysis reported reductions in nighttime crashes from 13% to 75% following new or improved lighting installations (Fotios & Gibbons, 2018). However, illumination alone does not fully explain crash risk. Many other factors contribute, including traffic volume, pedestrian activity, intersection design, and road geometry. Understanding the interplay between these variables is critical to developing safe and effective roadway lighting strategies.

At the same time, brighter lighting is not always better. Excessive street lighting or glare from vehicle headlights can reduce visibility and cause discomfort (Wood, 2020). Over-lighting also contributes to light pollution, which has been shown to disrupt circadian rhythms and negatively affect human health (Falchi et al., 2016; Khodasevich et al., 2020). Additionally, new technologies such as automatic emergency braking systems may be adversely affected by overly reflective materials and lighting conditions, leading to sensor confusion (Kidd & Spivey, 2024).

Balancing these competing goals—safety, environmental sustainability, and technological compatibility—requires a more nuanced approach to lighting design. Studies have shown that thoughtful outdoor lighting can promote not only safety but also broader quality-of-life benefits. For example, improved street lighting has been associated with increased pedestrian activity by reducing perceived insecurity (Painter, 1996), and women in particular consistently report feeling less safe in poorly lit areas (National Academies of Sciences & Medicine, 2011).

This project investigates how specific aspects of street lighting and intersection layout influence pedestrian visibility and safety in low-light conditions, while also accounting for the tradeoffs introduced by light pollution. Several factors can influence pedestrian visibility and, consequently, crash risk at night (see Table 1). In particular, it aims to characterize the safety and environmental performance of different lighting scenarios using photometric data and layout parameters (e.g., pole height, spacing, offset, and luminaire distribution). This work provides new insights to help transportation agencies make evidence-based decisions about lighting design that optimize both safety outcomes and sustainability.

2. Background and Literature Review

2.1. Pedestrian Fatality Statistics & Risk Factors

Pedestrian safety has become an increasingly urgent issue in the United States. In 2024, pedestrian fatalities reached 7,522—an average of 20 deaths per day. According to Smart Growth America (2025), this figure represents a 75% increase since 2010 and reflects the compounded effects of inequitable infrastructure conditions, including aging roadways, vehicle-centric design, and chronic underinvestment in lower-income communities. Vulnerable populations—including older adults, individuals with disabilities, and residents of low-income neighborhoods—are disproportionately impacted by this crisis.

Table 1. ***List of factors that can be used to model pedestrian lighting needs*** **(Vanasse Hangen Brustlin, Inc. et al., 2022).**

Group 1: Most common factors	Group 2: Less common factors	Group 3: Other factors
Average daily traffic (ADT) volumes	Available sight distance	Ambient lighting levels
Functional classification	Benefit-cost analysis	Frequency of inclement weather
Nearby development, land use, or density	Channelization devices (curb, guardrail, etc.)	Presence of parking
Night-to-day crash ratio	Intersection layout complexity	Retroreflective pavement markings (reduced need for lighting)
Night or pedestrian crash history	Presence of multiple turn lanes	Anticipated crossing locations for children (e.g., schools, parks, recreation centers)
Pedestrian/bike presence and crossing maneuvers (any, with or without marked crossings)	Speed limit (often 56+ or 72+ km/hr)	Speeding history (10+ mph over posted)
Pedestrian/bike volume during hours of darkness (often 100+/hr)	Vertical and horizontal curvature	Turning movement volumes
-	-	Wide or depressed medians

Data from the Governors Highway Safety Association (2024) indicate that the majority of pedestrian fatalities occur at night (see Figure 1) and frequently involve larger vehicles, such as light trucks and SUVs. A study conducted by the University of Wisconsin found that fatality rates spike approximately 20 to 50 minutes after sunset and remain elevated for several hours into the evening (Link, 2024). These findings are consistent with broader research linking elevated nighttime pedestrian risk to decreased visibility and inadequate lighting at intersections.

While studies by organizations such as the Insurance Institute for Highway Safety have demonstrated that pedestrian-activated or continuously illuminated crosswalks can improve driver yielding behavior (Hu et al., 2025), these interventions are typically evaluated in the context of midblock crossings. As such, they do not fully address the distinct visibility and safety challenges pedestrians face at signalized intersections.

2.2. Basic Terminology about Photometry of Urban Streetlighting

2.2.1. Illuminance

Illuminance refers to the amount of light falling on a surface and is measured in lux, defined as lumens per square meter. In low-light environments, streetlights provide the primary source of illumination necessary for drivers to detect road features, vehicles, intersections, and pedestrians—whether in crosswalks, waiting to cross, or walking along adjacent sidewalks. While vehicle headlights can contribute to pedestrian visibility, this lighting is intermittent and does not satisfy regulatory lighting requirements.

Illuminance is typically measured using three standard methods to capture different lighting conditions: horizontal, vertical, and semi-cylindrical. Horizontal and vertical illuminance are planar metrics, while semi-cylindrical illuminance adds a third dimension to better represent how pedestrians are perceived in space (see Figure 2). This third measurement is particularly valuable for assessing facial visibility and body contour recognition.

2.2.2. Luminance

Luminance refers to the amount of light reflected from a surface toward another surface. More specifically, it quantifies the intensity of light reflected from a surface per unit area in a given direction, and it is expressed in candelas per square meter (cd/m^2). Luminance is a key factor in determining how

Figure 1*. United States pedestrian fatalities by light condition.* (Governors Highway Safety Association, 2024)

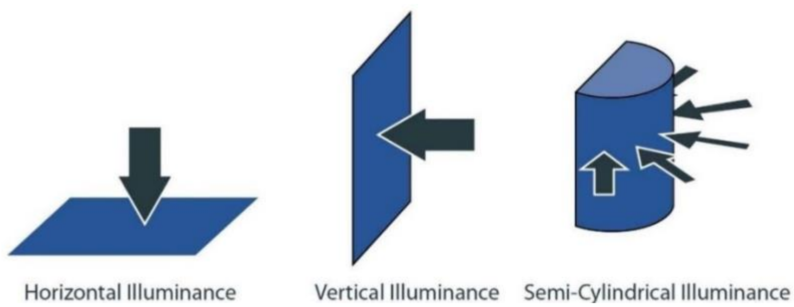

Figure 2. *Graphic methods of calculating illuminance* (Vanasse Hangen Brustlin, Inc. et al., 2022).

bright a surface appears to the human eye by quantifying how much light the surface reflects. For example, this metric explains why a light-colored surface appears brighter than a dark-colored surface under the same level of illuminance.

Light-emitting diode (LED) lights are brighter than older filament and most gas-discharge luminaires. Some LED streetlights can exceed 1,000,000 candelas (Miller, 2019). LEDs emit full-spectrum visual light, which contains a disproportionately high amount of blue light. Blue light scatters more than other wavelengths, giving the light a cooler white appearance. For instance, a 5,500K LED produces more blue light than sunlight at the same 5,500K color temperature. Color-correcting LEDs to 2,200K (similar to high-pressure sodium (HPS) lighting) or 2,700K (similar to candlelight) reduces the overall blue light output, but even then, it remains disproportionately greater than in HPS or other outdoor lighting sources.

In addition, luminance from surfaces—such as roadway and crosswalk striping—supplements the overall illuminance level. While not as intense as direct illumination, this reflected light can help illuminate parts of a pedestrian's body that may otherwise be poorly lit by overhead fixtures.

2.2.3. Glare

Glare refers to excessive brightness that impairs visibility. It occurs when a pedestrian can see the luminaire's light source while looking straight ahead toward the horizon. In the case of most streetlights, glare diminishes with distance and is not typically a concern for pedestrians standing directly beneath a

Figure 3. ***A photograph of streetlight glare*** **(Highways Industry, 2015).**

luminaire and looking forward. However, streetlights with flat diode arrays are more prone to producing glare, especially when the diodes are designed to project light across long distances. Raising the luminaire height or dimming the LEDs can reduce glare, but these adjustments are often not viable options at crosswalk intersections.

Glare can be categorized into three types (Figure 3):

- Nuisance glare is bothersome but mild; it can be avoided by looking away.
- Discomfort glare causes sustained visual strain but is not blinding. An example is crossing an intersection with the light source directly in the line of sight until reaching the area beneath the luminaire's 53° cone.
- Disability glare is more severe and occurs when one looks directly into the light source from a short distance, causing temporary blindness and a delay in visual recovery.

Glare becomes visible beyond the luminaire's 45° cone of useful light. For pedestrians, it typically becomes apparent at the 53° cone—the natural cutoff imposed by the forehead—and may extend as far as the 85° horizontal angle if the luminaire is extremely bright (Miller, 2019). For drivers, discomfort glare can be especially problematic when viewing a row of luminaires at low angles (between 75° and 90°) and without the ability to look away, such as when driving toward or alongside them.

Accurately quantifying glare remains a challenge due to the complexity of LED lighting systems (Miller, 2019). The Illuminating Engineering Society (IES) assesses glare using the Veiling Luminance Ratio (VLR), which evaluates how much a bright light source (measured vertically) impairs the eye's ability to perceive detail in the surrounding environment. A high VLR indicates increased glare and reduced visibility. Similarly, the International Commission on Illumination (CIE) developed a Glare Rating (GR) system in 1994, in which a higher number indicates more glare (CIE, 1994). These metrics and their application are further discussed in the Methodology section and summarized in Table 2.

2.2.4. Color Temperature

Early LED streetlights often emitted cooler color temperatures exceeding 4,000K correlated color temperature (CCT), intended to simulate daylight conditions (typically 5,500K–6,500K). However, these bright white lights frequently annoyed residents and led to their replacement with luminaires offering warmer color temperatures.

Table 2. ***Interpretation of GR from 10 to 90*** **(CIE, 1994).**

Interpretation	Glare rating (GR)
Unbearable	90
	80
Disturbing	70
	60
Just admissible	50
	40
Noticeable	30
	20
Unnoticeable	10

DarkSky International, a nonprofit advocating for the preservation of the night sky, strongly recommends maintaining a color temperature of 2,200K for all LED outdoor lighting. This warm yellow-orange light mimics HPS streetlights and minimizes the environmental and health impacts associated with blue light. DarkSky advises against the use of any outdoor lighting above 3,000K, which is considered the threshold for "warm" light before transitioning to "neutral" white.

Contemporary streetlights are available in 500K CCT increments, ranging from below 1,800K to the sunlight-equivalent 5,500K–6,500K range. When selecting a streetlight's color temperature, it is important to consider how blue light scattering affects both color perception and visual acuity. Cooler color temperatures enhance visual clarity and object detection, but they also contribute more to light pollution. Choosing a suitable color temperature for streetlighting therefore involves a trade-off among CCT, visibility, and environmental sustainability.

A study by the Virginia Tech Transportation Institute (VTTI) tested 2,200K, 4,000K, and 5,000K LED streetlights to evaluate driver visibility. In rural settings, the cool white 5,000K luminaire enabled pedestrian detection at distances up to 84m, while the neutral white 4,000K achieved 83m and the very warm white 2,200K reached 62m (Terry et al., 2020). The study also noted that in urban environments—with more ambient light and visual clutter—a higher luminance may be needed, especially to detect smaller pedestrians such as children.

Based on these findings, VTTI recommended the 4000K LED luminaire as an optimal compromise. It provided nearly equivalent visibility performance to the 5,000K model but with a reduced impact on light pollution. The report also concluded that a 3,000K color temperature would represent an acceptable minimum (Vanasse Hangen Brustlin, Inc. et al., 2022).

2.3. Streetlight Technologies and Concerns

Electronic lighting enables the individual management of LED streetlights when deployed as part of an interconnected, remotely managed communications system—typically via hardwired cabling or wireless networks such as Wi-Fi. This functionality is made possible by replacing the standard 3-pin photocell found on most streetlight luminaires with a 5- or 7-pin socket and a plug-in control module. With this upgrade, streetlights can be controlled either individually or in sub-groups, allowing local authorities to implement highly customized lighting strategies.

Control can be exercised centrally from a management center or locally in the field by authorized personnel, such as public safety officials, using a smartphone. Intersection and midblock crosswalk lighting can also be programmed independently or grouped as a subsystem within the broader lighting network. Current control functions typically include on-off switching, dimming capabilities, and performance

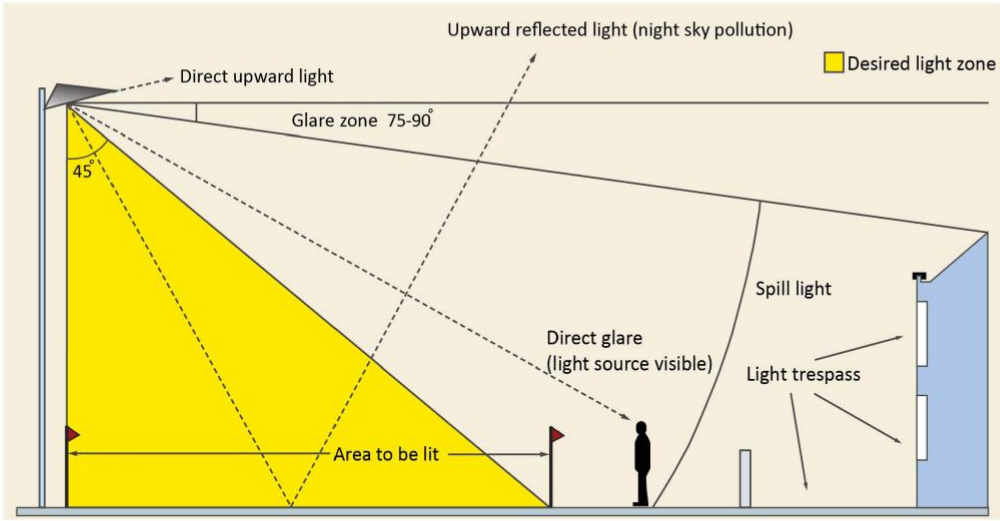

Figure 4. ***Glare and trespass conditions of light pollution*** **(DarkSky International, 2025).**

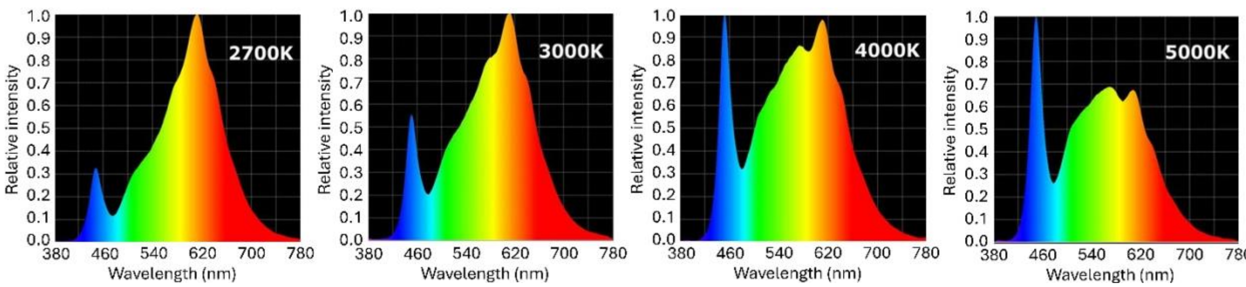

Figure 5. ***Blue light remains proportionally high at all color temperatures*** **(Baker, 2025).**

monitoring of individual luminaires. However, the same control modules can also support additional features such as environmental sensors, video surveillance, and other smart city functionalities.

The cost of adding this type of control module and communication system is significant—estimated at 75% to 100% of the cost of the luminaire itself (Remaking Cities Institute, 2016). One major environmental advantage of such systems is the ability to dynamically dim lighting. For instance, streetlights can operate at full brightness during active evening hours and later dim to minimum IES-compliant levels during periods of low vehicular traffic, reducing energy consumption and mitigating light pollution.

Streetlight ownership plays a critical role in how lighting systems are managed. Streetlights may be owned by local governments, utilities, or through shared arrangements. In some cases, local governments may own the luminaires but rent the poles from utilities and separately negotiate power rates. In others, the utility owns and manages the entire system, leaving local governments with little or no operational control. Limited government ownership can severely restrict the ability to implement responsive or adaptive streetlight management strategies.

Historically, roadway lighting has been designed primarily to support vehicle navigation, rather than to illuminate pedestrians at intersections. This vehicle-centric design legacy continues to limit the effectiveness of even high-performance fixtures in promoting pedestrian safety. While most jurisdictions have adopted LED cobrahead luminaires due to their energy efficiency, long service life, and compatibility with smart control systems, several key limitations persist.

2.3.1. Directional Limitations of LEDs

LEDs emit light in a directional manner, similar to individual flashlights. Unlike legacy lamps with curved, omnidirectional surfaces, LEDs project narrow beams of light, resulting in sharp cutoffs between illuminated and unilluminated areas (Baker, 2025). These focused beams often fail to evenly illuminate a pedestrian's full body, especially in cases where a person is standing directly under a luminaire but partially obscured—such as behind the luminaire's pole.

Although this directional quality can improve visibility for observers located in optimal positions, reflected luminance is still required to supplement direct illuminance in many areas. This limitation underscores the value of using the semi-cylindrical illuminance method, which accounts for three-dimensional lighting around the human form, rather than relying solely on traditional horizontal and vertical metrics. The semi-cylindrical method provides a more comprehensive understanding of how visible a pedestrian is within the lit environment.

2.3.2. Comfortability Concerns of LED Streetlights

The high brightness levels associated with LED luminaires can easily lead to glare and light trespass (see Figure 4). Even a few visible diodes can be distracting to pedestrians, and for individuals sensitive to bright lights, the intensity may cause discomfort or even temporary vision impairment. Drivers, in particular, may experience visual disruption from the bright luminance reflecting off road surfaces, especially when driving under streetlights that produce concentrated hotspots or when encountering strong contrast patterns from zebra-stripe crosswalks.

Even LEDs marketed as "warm white" tend to emit proportionally high levels of blue light compared to HPS or other traditional outdoor lighting sources (Baker, 2025). While LED lights can be engineered to match the visible spectrum of sunlight or moonlight, the proportion of blue light remains significantly higher at any given color temperature. This results in a cooler overall appearance, even for color temperatures that are nominally equivalent in Kelvin to warmer, traditional lighting sources (see Figure 5).

2.4. Pedestrian Lighting Design Metrics

The VTTI has served as an authority on pedestrian streetlighting research, producing several foundational reports for the Federal Highway Administration (FHWA). Three key publications formed the basis for the research presented in this report:

1. *Pedestrian Lighting Primer* (2022), developed in partnership with Vanasse Hangen Brustlin, Inc. and FHWA (Vanasse Hangen Brustlin, Inc. et al., 2022)
2. *Research Report: Street Lighting for Pedestrian Safety* (2020) (Terry et al., 2020)
3. *Safety Benefits and Best Practices for Intersection Lighting* (2020) (Li et al., 2020)

The *Pedestrian Lighting Primer* synthesized VTTI's research alongside guidance from several other authoritative sources, including:

- The *AASHTO Roadway Lighting Design Guide*, 7th Edition (AASHTO, 2018)
- The *Transportation Association of Canada (TAC) Guide for the Design of Roadway Lighting* (TAC, 2006)
- *NCHRP Report 152: Warrants for Highway Lighting* (TRB, 1974)
- *Illuminating Engineering Society (IES) RP-8-18: Recommended Practice for Design and Maintenance of Roadway and Parking Facility Lighting* (IES, 2018)

- FHWA's *Informational Report on Lighting Design for Midblock Crosswalks* (Vanasse Hangen Brustlin, Inc. et al., 2022)

Together, these documents establish a comprehensive framework for evaluating lighting requirements for pedestrian facilities, both at intersections and midblock crossings. In Table 3, we compile the regulatory requirements and design recommendations drawn from the VTTI publications used in this study. These include considerations for pedestrian zones such as crosswalks, sidewalks, and intersection corners.

To contextualize roadway classification and pedestrian volume, the *Pedestrian Lighting Primer* also presents a reference table (see Table 4) that merges ANSI/IES RP-8-18 intersection lighting standards with three roadway classifications—major, collector, and local—based on average daily pedestrian traffic volumes (categorized as high, medium, or low).

In order to evaluate whether streetlights alone can satisfy both pedestrian- and vehicle-focused lighting requirements, VTTI identified key design targets that should be met in lighting simulations (Vanasse Hangen Brustlin, Inc. et al., 2022):

1. Crosswalks at intersections should provide a vertical illuminance of 30 lux, while midblock crosswalks require 20 lux. Both scenarios assume LED luminaires with a CCT between 3,000K and 4,000K.

2. Pedestrian facilities adjacent to roadways are evaluated based on pedestrian activity levels:
    - For low to medium pedestrian activity (fewer than 100 pedestrians per hour (PPH)):
        - Vertical illuminance: 2 lux
        - Urban luminance target: 1 cd/m²
        - CCT: 3,000K to 4,000K
    - For high pedestrian activity areas or school zones (more than 100 PPH):
        - Semi-cylindrical illuminance: 10 lux
        - Rural luminance: 1 cd/m²
        - Urban luminance: 2 cd/m²
        - CCT: 3,000K to 4,000K

These targets are based on roadway-scale luminaires mounted at heights of 6.5m or greater. For pedestrian-scale lighting mounted below 6.5m, additional thresholds apply: an increase of 2 lux in illuminance and 0.5 cd/m² in luminance is recommended to counteract the effects of glare.

2.5. Design Configurations

Much of the recent literature—particularly research authored by the VTTI—has focused on optimizing lighting configurations to improve pedestrian visibility at midblock crosswalks (Gibbons et al., 2008; Terry et al., 2020). From these studies, three dominant lighting configurations have emerged (see Figure 6).

Note: While these configurations were primarily developed for midblock crossings, this report focuses on their applicability and limitations for intersection streetlight design.

Table 3. ***A summary of pedestrian crosswalk lighting requirements and recommendations compiled from VTTI studies.***

Item	Location	FHWA requirements	ANSI/IES RP-8-18 requirements	VTTI and other source recommendations
Intersection illuminance (see Table 4 for details)	For intersections, the recommended illumination level is determined by summing the lighting levels of each roadway entering the intersection, based on their classification by ADT. Major Roadway (Arterial): ADT > 3,500. Collector Roadway: ADT between 1,500 and 3,500. Local Roadway: ADT < 1,500. The total recommended illumination at an intersection is the sum of the required levels for each entering roadway, as defined by IES guidelines.		18–34 lux Major/ Major 15–29 lux Major/Collector 13–26 lux Major/Local 12 – 24 lux Collector/Collector 10 – 21 lux Collector/Local 8 – 18 lux Local/Local	
Midblock pedestrian crossing illuminance			50% higher illuminance than required for the roadway	
Pedestrian illuminance	Intersection crosswalks at 1.5m height	30 lux vertical average across the center of the marked crosswalk measured at <2m increments		40 lux vertical average recommended by VTTI measured across the center of the marked crosswalk measured at <2m increments to overcome strong ambient lighting in urban locations
	Midblock crosswalks at 1.5m height	20 lux vertical average across the center of the marked crosswalk measured at <2m increments	20 lux vertical average across the center of the marked crosswalk measured at <2m increments	
	Adjacent pedestrian facilities at 1.5m height: Pedestrian high volume (>100 PPH)	10 lux semi-cylindrical average across the center of the pathway measured at <2m increments		
	Adjacent pedestrian facilities at 1.5m height: Pedestrian low to medium volume (<10 to 100 PPH)	2 lux semi-cylindrical average across the center of the pathway measured at <2m increments		
Pavement luminance (see Table 4 for details)	Roadways		IES RP-8-18 Table 2 (L average cd/m^2) depending on street classification.	
	Adjacent pedestrian facilities: (Urban) pedestrian high volume		IES RP-8-18 Table 2 depending on street classification: (Urban)	

	(>100 PPH measured at <2m increments)		2.0 cd/m^2 average; (Rural) 1 .0 cd/m^2 average	
	Adjacent pedestrian facilities: (Rural) pedestrian low to medium volume (<10 to 100 PPH measured at <2m increments)		IES RP-8-18 Table 2 depending on street classification: (Urban) 1.0 cd/m^2 average; (Rural) use typical road luminance requirements	
CCT light source and pedestrian detection distances from vehicle in rural setting	2,200K CCT			0.5–1.0 cd/m^2 at about 62m average distance
	4,000K CCT			0.5, 1.0, and 2.0 cd/m^2 at about 83m average distance 4,000K CCT recommended as little difference from 5,000K CCT. 3,000K CCT is an acceptable minimum.
	5,000K CCT			0.5, 1.0, and 2.0 cd/m^2 at about 84m average distance
Uniformity ratio (Contrast) **Two types: Positive contrast (pedestrian brighter); negative contrast (pedestrian in silhouette) (see Table 4 for details)**	Intersections in urban settings. Positive contrast recommended. IES contrast type dependent on roadway Intersection types.	Positive contrast illuminance	Positive contrast illuminance. 3 Major/Major 3 Major/Collector 3 Major/Local 4 Collector/Collector 4 Collector/Local 6 Local/Local	
	Midblock in all locations. Positive contrast recommended.		Positive contrast illuminance. 3 Major 4 Collector 6 Local	
Glare (Veiling luminance) (see Table 4 for details)	Veiling luminance location where disability glare occurs		IES RP-8-18 maximum allowable using flat glass lumens parallel to road surface	Pedestrian glare issue when light source height <6.5m
Light trespass			Maximum allowable levels based on environmental zone ratings (IES, 2018)	
Pole height and pedestrian/object detection distances from vehicle	Roadway scale luminaires >6.5m			0.5 cd/m^2 = 53m 1.0 cd/m^2 = 50m 2.0 cd/m^2 = 58m
	Pedestrian scale luminaires <6.5m			0.5 cd/m^2 = 57m 1.0 cd/m^2 = 63m 2.0 cd/m^2 = 65m
Light loss factor due to deterioration	Apply to each luminaire's IES file			0.85
Crosswalk entry area lighting	Below the pole			Some Department of Transportations (DOTs) require a 1.5m lit radius

Pole location	Intersection: Before crosswalk on the vehicle approach side	Some DOTs require distance of 0.5x to 1.0x the pole height measured from vehicle approach front edge of the crosswalk
	Midblock: Before crosswalk on the vehicle approach side	Some DOTs require a distance of 0.5x to 1.0x the pole height measured from vehicle approach edge of the crosswalk
Surround ratio (% average illuminance of backlighting)	Average illuminance in the area adjacent to a roadway equal in width to a travel lane compared to the average illuminance of the roadway	>80%

- Dynamic (or Box) Configuration: This approach uses four poles positioned at each corner of the intersection, aiming inward. While the layout offers symmetry, it often fails to effectively illuminate pedestrians from the perspective of approaching drivers. It also may inadequately light vehicle turning paths.
- Midblock Staggered Configuration: In this setup, poles are positioned in advance of the crosswalk—one on each side. This arrangement provides strong pedestrian illumination and visual contrast from the driver's perspective. However, it is poorly suited for intersections due to limited coverage of multiple approach paths.
- Turbine Configuration: Four poles are installed forward of the intersection, oriented to light pedestrians in the approach path of oncoming vehicles. This configuration has been found effective for frontal pedestrian visibility but tends to perform poorly for illuminating sidewalk approaches or pedestrians crossing from side angles.

VTTI's simulation studies, which used manufacturer-provided IES photometric files, found the turbine configuration—when paired with 4,000K LEDs, Type II beam distribution (see Figure 7), and lower pole heights (approximately 9.1m)—was the most effective layout for meeting ANSI/IES RP-8-18 vertical illuminance targets at intersections. However, even this configuration does not guarantee full-body illumination of pedestrians from all approach angles, especially those relevant to turning vehicles.

Across all configurations, performance is highly sensitive to pole spacing, orientation, height, and wattage. The most effective designs placed poles at a distance 0.5x to 1.0x their mounting height in advance of the crosswalk. Simulation findings also showed that increasing wattage (from 204W to 268W) or lowering pole height (from 10.7m to 9.1m) can help bridge the gap between standard compliance and recommended lighting performance.

Nonetheless, these strategies come with tradeoffs. Higher wattage and lower pole heights may increase energy use, raise maintenance costs, and contribute to light pollution. These findings underscore the need for new tools and metrics that support a holistic evaluation of streetlight configurations, balancing safety, energy efficiency, and environmental sustainability.

Table 4. ***Recommended roadway luminance criteria by street classification and pedestrian activity*** **(from IES RP-8-18, not required by FHWA regulations) (Vanasse Hangen Brustlin, Inc. et al., 2022).**

Street classification	Pedestrian activity classification	Average luminance L_{avg} (cd/m²)	Average uniformity ratio $L_{\text{avg}}/L_{\text{min}}$	Maximum uniformity ratio $L_{\text{max}}/L_{\text{min}}$	Maximum veiling luminance ratio $L_{\text{v,max}}/L_{\text{avg}}$
Major	High	1.2	3.0	5.0	0.3
	Medium	0.9	3.0	5.0	0.3
	Low	0.6	3.5	6.0	0.3
Collector	High	0.8	3.0	5.0	0.4
	Medium	0.6	3.5	6.0	0.4
	Low	0.4	4.0	8.0	0.4
Local	High	0.6	6.0	10.0	0.4
	Medium	0.5	6.0	10.0	0.4
	Low	0.3	6.0	10.0	0.4

Note: L_{avg}: Maintained average pavement luminance; L_{min}: Minimum pavement luminance; $L_{\text{v,max}}$: Maximum veiling luminance

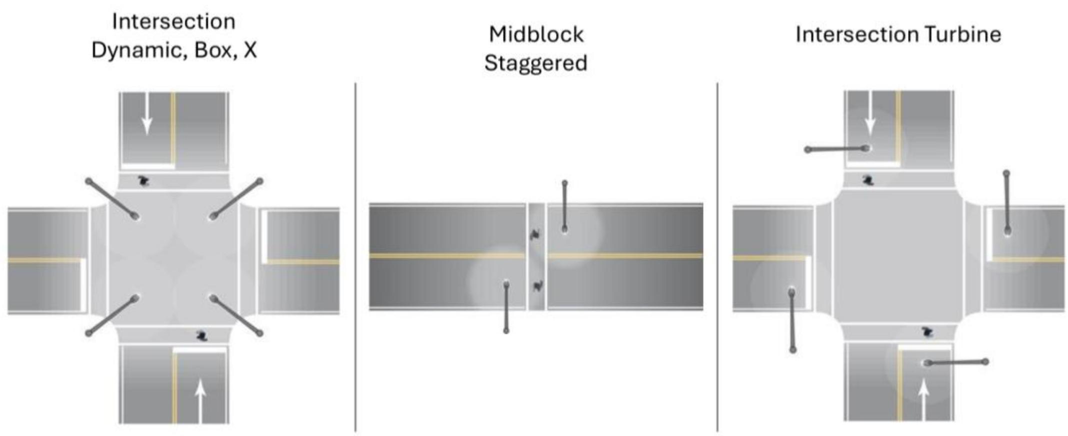

Figure 6. ***Diagrams of pole and luminaire locations for crosswalk configurations*** **(Gibbons et al., 2008).**

2.6. Research Questions

Given the increasing complexity of lighting design for urban intersections—particularly under the dual mandates of enhancing pedestrian safety and minimizing environmental impact—this study addresses two central research questions:

1. ***How does the combination of light source characteristics and streetlight geometry influence overall design performance for pedestrian visibility at intersections?***

Rather than assessing lighting parameters or spatial configurations in isolation, this study examines how specific combinations—such as beam distribution type paired with pole orientation or spacing—collectively affect critical performance metrics. These include vertical illuminance, semi-cylindrical illuminance, glare, and luminance. This approach allows for a more integrated evaluation of design effectiveness.

Key sub-questions include:

- *Can Type III or Type IV luminaires meet FHWA and ANSI/IES RP-8-18 pedestrian illuminance criteria?*

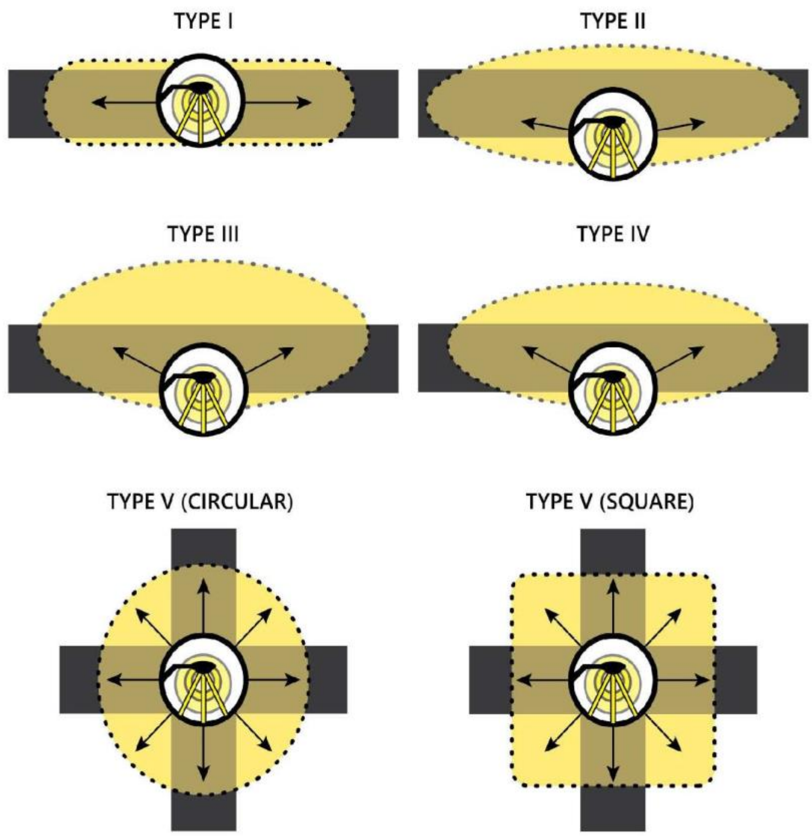

Figure 7. ***Representation of IES distribution types*** **(modified from IES RP-8-19) (Vanasse Hangen Brustlin, Inc. et al., 2022).**

- *Can semi-cylindrical illuminance satisfy the 30 lux vertical illuminance minimum, as well as VTTI's recommended 40 lux vertical illuminance target for urban intersection crosswalks?*

2. Do lighting configurations that perform well for pedestrian safety also meet acceptable thresholds for minimizing light pollution and visual discomfort?

While some lighting designs achieve strong safety performance, they may also introduce unintended consequences—such as excessive glare or elevated skyglow. This study explores whether high-performing configurations, such as turbine layouts, can meet pedestrian visibility standards and remain within acceptable environmental and visual comfort limits. In doing so, the research seeks to determine whether a balanced solution can be achieved that supports both safety and sustainability objectives.

3. Methodology

To evaluate how combinations of light source characteristics and streetlight placement influence intersection lighting performance—particularly in relation to pedestrian safety and light pollution—this study developed and applied a custom, Python-based simulation toolkit: SALUSLux. The toolkit is available open-source at: https://github.com/CMU-SALUS-Lab/saluslux.

SALUSLux was created to address major limitations in existing commercial lighting design tools such as DIALux and ReLux. These tools are widely used for architectural visualization and lighting simulation but have two key drawbacks:

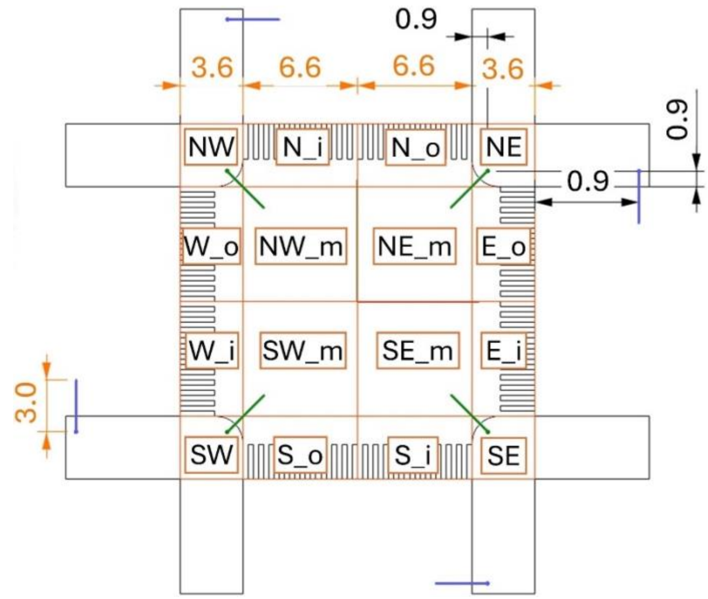

Figure 8. ***Overall dimensions of the intersection considered in the case study (all units in meters). Each surface is labeled using the cardinal directions, with suffixes denoting respective roles: _i for incoming, _o for outgoing, and _m for middle of the intersection. The 45° turbine configuration is shown in green, and the 90° turbine configuration is shown in blue. The street width is 6.6m on each side of traffic (or 3.3m per lane).***

1. Limited compatibility with standard photometric file formats: While the IES maintains an accessible, plain-text format for photometric data (ANSI/IES LM-63-19), many commercial tools restrict its use—accepting only proprietary formats (e.g., Unified Luminaire Data or ULD in DIALux) unless users upgrade to paid versions. Most lighting manufacturers continue to distribute photometric data primarily in the IES format, making this a substantial barrier for accessibility and transparency.
2. Emphasis on manual rendering over programmatic control: Mainstream tools prioritize 3D modeling via graphical user interfaces, making it difficult to systematically vary lighting parameters such as pole height, spacing, distribution type, and color temperature. This approach is impractical for simulating large numbers of design alternatives or optimizing for multiple, interacting criteria such as illuminance, glare, and environmental sustainability.

To overcome these constraints, SALUSLux was built using Python and designed to support parametric, reproducible, and large-scale lighting simulation. It allows researchers and practitioners to load standard IES files, define streetlight configurations programmatically, and simulate lighting behavior across a wide range of design parameters. These include pole height, mounting offset, orientation, luminaire distribution type, wattage, and color temperature—enabling scalable analysis that would be time-prohibitive using traditional tools.

3.1. Simulation Setup

The simulation model represents a standard four-way North American intersection, with four lanes per leg. The intersection layout is divided into 16 calculation surfaces, including inbound and outbound crosswalks, lane interiors, and central intersection zones (see Figure 8). This segmentation allows for surface-specific lighting assessments, including:

- Facial visibility at crosswalk entry points

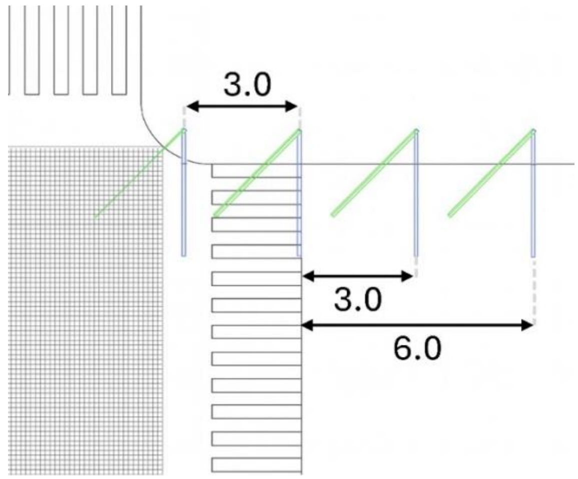

Figure 9. ***Schematic showing different offset variations, in this case, for a height of 6m (all units in meters).***

- Glare exposure in vehicle approach zones
- Lighting uniformity across driving and walking surfaces

Each simulation scenario combined the following components:

1. Pole placement configuration (2 options):
    - 90° Turbine Configuration: Four poles placed at the intersection corners, each aimed orthogonally toward the center (0°, 90°, 180°, 270°), shown in blue.
    - 45° Turbine Configuration: Four poles positioned diagonally, aimed inward toward the center (45°, 135°, 225°, 315°), shown in green.
2. Offset-to-height ratio (4 levels): Also referred to as the "offset-to-z" ratio, this variable determines how far each pole is placed from the corner, relative to its mounting height. Ratios of 0.0×, 0.5×, 1.0×, and 1.5× were tested (see Figure 9).
3. Pole mounting height (4 levels): Simulations were conducted at heights of 6.0m, 6.5m, 7.0m, and 7.5m.
4. Lighting system configuration, composed of:
    - 4 IES distribution types: Type II, III, IV, and V
    - 3 wattage levels: Nominal 50W, 100W, and 150W
    - 3 color temperatures: 2700K, 3000K, and 4000K
    - 2 lighting manufacturers: Representing different real-world luminaire designs

This setup resulted in:

(2 configurations × 4 offsets × 4 heights) × (4 types × 3 wattages × 3 CCTs × 2 manufacturers) =

2,304 simulation scenarios

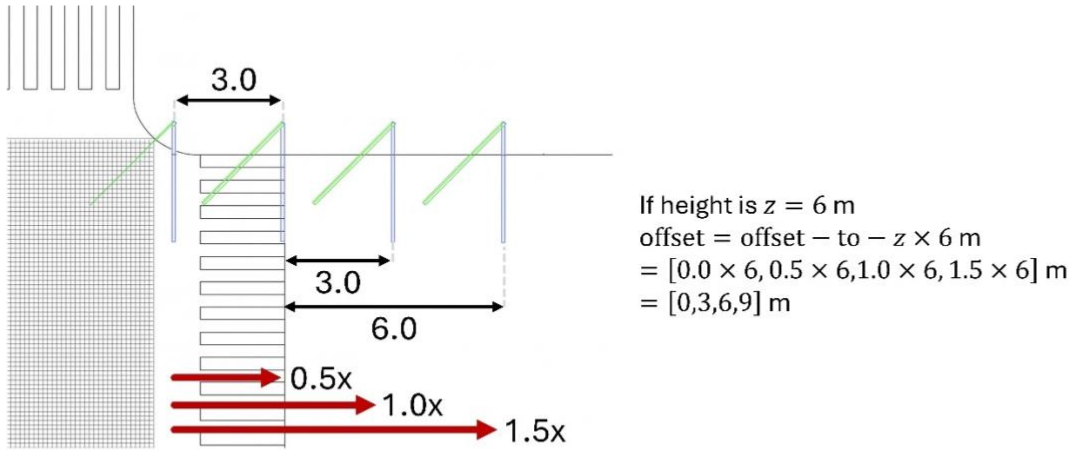

Figure 10. ***An example of the steps to make new coordinates based on a set of offset ratios.***

By systematically exploring this multidimensional design space, the study evaluated how different combinations of physical layout and lighting parameters influence key performance metrics such as vertical illuminance, semi-cylindrical illuminance, glare, and luminance. The use of SALUSLux enabled automation, repeatability, and scalability, providing a unique capability to analyze and balance competing design goals in pedestrian lighting—particularly at complex urban intersections.

3.1.1. Scenario Input Generation Process

The process of generating simulation scenarios began by defining the full range of design parameters, starting with pole heights. The study incorporated 32 IES photometric files, evenly split between two lighting manufacturers: Lumec (16 files) and Cooper (16 files). The directory paths for each file were cataloged during this setup phase.

Next, the pole layouts for each configuration were defined by specifying the initial (x,y) coordinates of the four poles and their orientation angles. Orientation followed standard mathematical convention, where 0° corresponds to the positive x-axis and increases in the counterclockwise direction. The origin point (0, 0) was fixed at the center of the intersection to serve as the reference for all pole placements.

For the 90° configuration:

```
coords: [(10.2, 7.5), (-7.5, 10.2), (-10.2, -7.5), (7.5, -10.2)],
orientations: [270°, 0°, 90°, 180°]
```

For the 45° configuration:

```
coords: [(-7.5, 7.5), (7.5, 7.5), (-7.5, -7.5), (7.5, -7.5)],
orientations: [315°, 225°, 45°, 135°]
```

A Python script was developed to automatically iterate over all combinations of simulation parameters using a nested loop structure. Specifically, the script iterated through:

- 4 values of pole height,

- 4 values of offset-to-height (offset-to-z) ratio,
- 32 IES files,
- and 2 pole configurations (90° and 45° turbine layouts).

For each iteration, the script calculated the actual offset distance and determined the new pole positions using basic trigonometry. Each pole's location was updated by shifting it outward from the intersection center along its designated orientation angle (θ). The updated coordinates for each pole were computed as:

$$x = x_0 + \text{offset} \cdot (-\sin(\theta)), \qquad y = y_0 + \text{offset} \cdot \cos(\theta)$$

Here, x_0, y_0 represent the pole's base position, and θ is the orientation angle for that specific light in the layout. Figure 10 illustrates this geometric offset process.

For the 90° turbine configuration, pole locations were aligned with zebra crosswalks. These locations were later used as a basis for comparison with the 45° layout in expanded design iterations.

Each simulation scenario was encoded in a CSV file with four rows—one for each of the four poles. Each row included the following columns:

- `scenario_name`: A unique identifier for the scenario
- `light_id`: Identifier for the individual pole (1–4)
- `x`, `y`: Computed pole coordinates
- `z`: Pole mounting height
- `orientation`: Luminaire orientation in degrees
- `ies_file`: File path to the corresponding IES file
- `config`: Configuration type (e.g., 90° or 45° turbine)
- `offset_to_z_ratio`: The ratio of lateral offset to pole height

All scenarios were written to a single file, `scenarios.csv`. This automated process replaced what would otherwise have been a tedious and error-prone task of manually enumerating thousands of configuration combinations. The resulting structured dataset was then used as input for batch simulation and performance evaluation in SALUSLux.

3.2. SALUSLux Software

We begin by defining a modular set of functions within the SALUSLux library, each corresponding to core calculations typically required in professional lighting design workflows. The remainder of this section outlines the structure of the software and key modeling assumptions.

3.2.1. Parsing IES Photometric Files

The first major module of the SALUSLux software is responsible for parsing IES photometric files, which are standardized data formats published by lighting manufacturers. These files contain detailed information—such as luminous intensity measurements and metadata—that is essential for performing accurate lighting simulations. Although IES files are stored as plaintext, programmatic parsing presents challenges due to inconsistent formatting practices across manufacturers.

3.2.1.1. Metadata Extraction

The parsing process begins by reading the IES file line-by-line to extract relevant metadata fields. These typically include the number of lamps, lumens per lamp, candela multiplier, ballast factor, input wattage, and physical dimensions of the fixture. Most of these fields appear in consistent locations as defined by the ANSI/IES LM-63 specification. However, not all useful information is explicitly encoded within the file. For instance, the luminaire's distribution type (e.g., Type II, III, IV) is often not included as a data field. Instead, manufacturers frequently include this information in the file name, requiring the use of regular expressions and heuristics to infer the intended distribution type when it is absent from the body of the file.

3.2.1.2. Luminous Intensity Distribution

Once the metadata is parsed, the next step is to extract the luminous intensity distribution. This is represented over a grid of horizontal angles $\boldsymbol{H} = [h_1, h_2, \ldots, h_{n_H}]$ and vertical angles$\boldsymbol{V} = [v_1, v_2, \ldots, v_{n_V}]$, where n_H and n_V are the number of angles in each dimension. Because of symmetry, many IES files define only a portion of the total angular range—for example, a quarter or half of the full 360° horizontal or 180° vertical sweep.

To reconstruct the full light distribution, SALUSLux mirrors and concatenates the input angles to produce a complete representation. For quarter-symmetric files, horizontal angles are expanded as:

$$\boldsymbol{H}_{\text{full}} = [\boldsymbol{H}, 180^\circ \cdot \boldsymbol{1} - \boldsymbol{H}_{\text{rev}}, 180^\circ + \boldsymbol{H}, 360^\circ - \boldsymbol{H}_{\text{rev}}]$$

For half-symmetric files, the horizontal domain is completed using:

$$\boldsymbol{H}_{\text{full}} = [\boldsymbol{H}, 360^\circ - \boldsymbol{H}_{\text{rev}}]$$

In both cases, $\boldsymbol{H}_{\text{rev}}$ refers to the reversed sequence of input horizontal angles, and $\boldsymbol{1}$ is a vector of ones. Vertical angles are mirrored similarly to generate the full 180° hemispherical distribution.

For example, an IES file that specifies angular data from 0°–90° vertically and 0°–180° horizontally (V90–H180) will be extended to a full V180–H360 configuration. This ensures that light output can be simulated in all directions.

3.2.1.3. Candela Matrix Construction

The luminous intensity values—reported in candelas—are parsed into a two-dimensional matrix $\boldsymbol{C}$, where each element $C_{ij} = I(h_i, v_j)$ corresponds to the light intensity at a specific horizontal and vertical angle pair. This matrix serves as the foundational dataset for all subsequent illumination calculations in the SALUSLux framework.

3.2.1.4. Angular Interpolation

Since IES files only specify intensities at discrete angle intervals, SALUSLux uses interpolation to estimate intensity values at arbitrary directions in 3D space. This is accomplished using bilinear interpolation via SciPy's `RegularGridInterpolator` (Virtanen et al., 2020). This allows smooth and continuous estimation of luminous intensity from the discrete angle grid.

At any given horizontal angle ϕ and vertical angle θ, the interpolated intensity is defined as:

$$I(\phi, \theta) = \text{interp}(\phi, \theta; \boldsymbol{H}, \boldsymbol{V}, \boldsymbol{C})$$

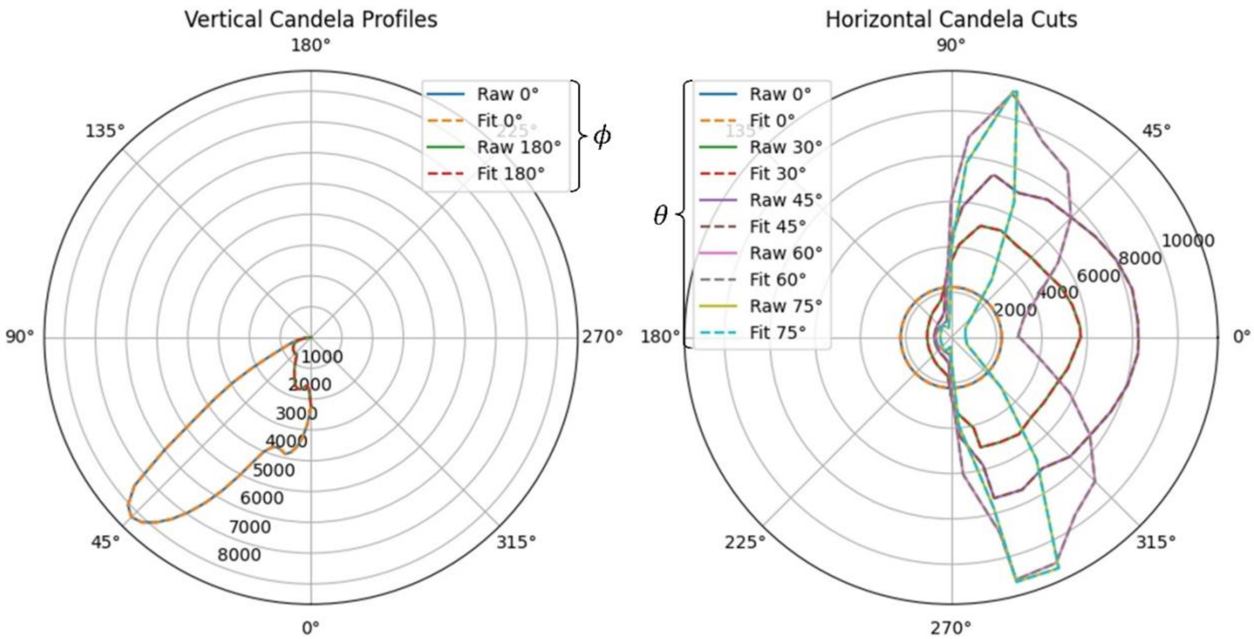

Figure 11. ***A pair of polar plots from an IES file, with (left) a plot of candela values at each vertical angle (i.e., a side view of light), and (right) a plot of candela values at each horizontal angles (i.e., a top view of light). Each plot is shown together with their interpolations.***

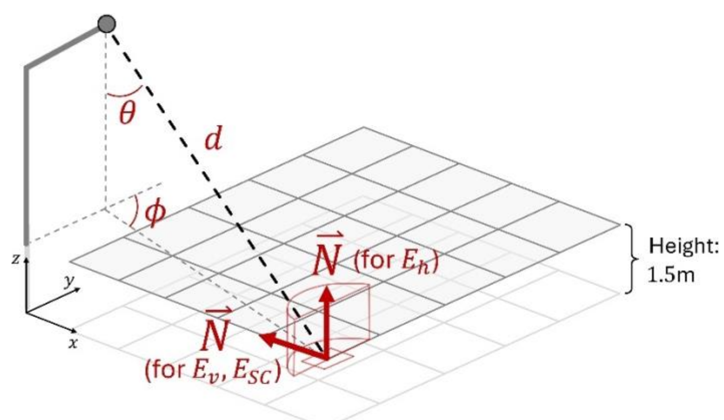

Figure 12. ***Basic illumination geometry assigns a normal vector $\vec{N}$ at each point to compute the lux received from a streetlight based on position and orientation*** **(Kavee at al., 2025)*.***

Here, θ represents the angle from the vertical axis (surface normal), and $\phi$is the azimuthal angle in the luminaire's coordinate system.

If the parsed IES file includes a non-unity candela multiplier, all entries in the intensity matrix $\boldsymbol{C}$ are scaled accordingly:

$$\boldsymbol{C}_{\text{scaled}} = \boldsymbol{C} \times \text{candela multiplier}$$

This interpolation process is critical for accurately simulating how light behaves in a spatially continuous environment—particularly when calculating performance metrics such as illuminance, luminance, and glare.

3.2.2. Generating Evaluation Grid Points

To evaluate spatial patterns of lighting coverage, SALUSLux includes a function called `generate_unified_grid`, which constructs a mesh of evaluation points across a user-defined rectangular domain. The grid spans a planar region bounded by:

$$x_{\min} \leq x \leq x_{\max}, \qquad y_{\min} \leq y \leq y_{\max}$$

The vertical coordinate is fixed at $z = 0$, representing ground level.

Given a user-specified grid resolution, this function calculates the (x, y, z) coordinates of each evaluation point within the domain. The resulting grid serves as a spatial sampling surface for computing lighting metrics, such as illuminance or glare, and enables visualization of lighting performance across the entire intersection or pedestrian zone. This uniform grid acts as the foundation for analyzing how different lighting configurations affect coverage, uniformity, and pedestrian visibility across various surfaces of interest.

3.2.3. Computing Illumination

Illuminance, expressed in lux, represents the amount of light striking a surface and is a key determinant of visibility, facial recognition, and perceived safety—particularly in pedestrian environments. This module in SALUSLux implements two core illuminance metrics widely used in lighting design. Planar illuminance, which is calculated on flat surfaces and includes horizontal illuminance, E_h, and vertical illuminance, E_v. Semi-cylindrical illuminance, E_{sc}, is a metric that approximates light distribution around a vertical cylindrical surface—useful for capturing light falling on the contours of the human body, including facial features and side illumination. By supporting both planar and semi-cylindrical calculations, this module provides a more comprehensive analysis of lighting performance in pedestrian-focused settings. These metrics are computed at each point on the evaluation grid, enabling detailed spatial assessment of lighting quality across intersection surfaces.

3.2.3.1. Planar Illuminance

The function `compute_illuminance` calculates the illuminance at each evaluation grid point by using the luminous intensity $I(\phi, \theta)$ emitted from a luminaire positioned at coordinates $L(x_L, y_L, z_L)$ (Figure 11). The calculation is based on the standard photometric equation:

$$E(\vec{N}) = \frac{I(\phi, \theta)\cos(\theta)}{d^2}$$

Here, d is the distance between the light source and the evaluation point:

$$d = \sqrt{(x - x_L)^2 + (y - y_L)^2 + (z - z_L)^2}$$

The cosine of the angle θ between the light direction and the surface normal is computed as:

$$\cos(\theta) = \frac{\vec{N} \cdot (-\vec{L})}{|\vec{L}|}$$

In this expression, $\vec{N}$ is the unit surface normal vector (e.g., upward for horizontal illuminance E_h), and $\vec{L}$ is the vector from the luminaire to the point of interest. Figure 12 illustrates this geometry.

By default, SALUSLux evaluates illuminance at a height of 1.5m above the ground—a standard height recommended in transportation lighting guidelines (Vanasse Hangen Brustlin, Inc. et al., 2022). This elevation represents a compromise between a driver's line of sight and a pedestrian's face height, making it a practical reference point for assessing nighttime visibility in urban intersections. This height can be adjusted by the user to reflect alternative modeling scenarios.

3.2.3.2. Semi-Cylindrical Illumination

In addition to planar (horizontal and vertical) illuminance, SALUSLux includes functionality to compute semi-cylindrical illuminance E_{sc}, which captures light incident from a range of horizontal directions. This metric is particularly important for evaluating pedestrian visibility from multiple viewing angles, such as those encountered by drivers approaching from different lanes or turning paths.

The function `compute_illuminance_sc` estimates semi-cylindrical illuminance by averaging planar illuminance values across a set of rotated surface normal $\vec{D}_i$, simulating lateral incident angles:

$$E_{sc}(\vec{N}) = \frac{1}{n}\sum_{i=1}^{n} E(\vec{D}_i)$$

Each direction $\vec{D}_i$ is calculated by rotating the original surface normal vector $\vec{N}$ by a horizontal angle α_i:

$$\vec{D}_i = \begin{bmatrix} \cos(\alpha_i) & -\sin(\alpha_i) \\ \sin(\alpha_i) & \cos(\alpha_i) \end{bmatrix} \begin{bmatrix} N_x \\ N_y \end{bmatrix}$$

Here, N_x and N_y are the x- and y-components of the surface normal vector. By default, SALUSLux samples from a set of nine angles:

$$\alpha_i = \{-90°, -45°, 0°, 45°, 90°\}$$

This approach ensures that visibility from a range of typical driver approach directions is still captured while maintaining computational efficiency.

3.2.4. Computing Luminance

In addition to calculating illuminance, SALUSLux also supports the computation of luminance, a photometric quantity that more directly reflects how bright a surface appears to a human observer. While illuminance measures the amount of light incident on a surface, luminance quantifies the portion of that light that is reflected toward an observer.

Formally, luminance is defined as the radiant intensity per unit projected area per unit solid angle (MacEvoy, 2025; Ossila, 2025):

$$L = \frac{d^2\Phi}{dA \cdot d\omega \cdot \cos(\theta)}$$

Where $d^2\Phi$ is the differential luminous flux reflected from the surface, dA is the differential surface area, $d\omega$ is the differential solid angle subtended by the viewer's direction, and θ is the angle between the surface normal and the observer's line of sight.

Because luminance depends on the reflective properties of the surface, SALUSLux adopts a Lambertian reflection model. This model assumes that surfaces reflect light diffusely and uniformly in all directions, as opposed to specular (mirror-like) reflections. This is a common and practical assumption for materials such as asphalt and concrete in transportation settings.

To derive a working formula for luminance under Lambertian conditions, we begin by integrating the total reflected flux Φ over a hemisphere, using spherical coordinates:

$$\Phi = \int_0^{2\pi} \int_0^{\pi/2} L \cdot \cos(\theta) \cdot \sin(\theta)\, d\theta d\phi$$

The azimuthal integration over ϕ yields a factor of 2π, and the polar integral evaluates to:

$$\int_0^{\pi/2} \cos(\theta) \cdot \sin(\theta)\, d\theta = \frac{1}{2}$$

Combining these results gives:

$$\Phi = L \cdot 2\pi \cdot \frac{1}{2} = L \cdot \pi \rightarrow L = \frac{\Phi}{\pi}$$

To compute Φ, we use the surface reflectance factor ρ and the illuminance E, such that:

$$\Phi = E \cdot \rho \rightarrow L = \frac{E \cdot \rho}{\pi}$$

This expression enables SALUSLux to compute luminance from illuminance values using a specified reflectance. For typical asphalt road surfaces, a default reflectance of 20% is used, consistent with empirical studies of spectral surface reflectivity (Singh & Garg, 2013). The resulting luminance values are critical for evaluating glare potential, a key component of visual comfort and safety in nighttime driving and pedestrian environments.

3.2.5. Computing Glare Rating

Glare is a crucial consideration in nighttime lighting design, as excessive brightness can impair visibility, cause discomfort, and obscure important visual cues—particularly those related to pedestrian presence and movement. To quantify glare, SALUSLux includes a `compute_glare_rating` function that implements the GR metric defined by the CIE standard (CIE, 1994).

The GR at a given observer viewpoint is computed using the following expression:

$$GR(\vec{N}) = 24 + 27 \log_{10}\left(\frac{L_{VL}}{L_{VE}^{0.9}}\right)$$

In this equation, L_{VL} is the veiling luminance caused by direct exposure to bright luminaires within the observer's field of view. L_{VE} represents the environmental veiling luminance, accounting for background adaptation and ambient brightness. Veiling luminance L_{VL} is estimated based on the vertical illuminance at the observer's eye, contributed by nearby luminaires at angular distances q_i ranging from 1.5° to 60° from the direction of view. It is calculated as:

$$L_{VL} = 10 \sum_i \frac{E_i(\vec{N}_{q_i})}{q_i^2}$$

Here, $E_i(\vec{N}_{q_i})$ is the vertical illuminance at the observer's eye from luminaire i and q_i is the angle between the viewing direction and the luminaire's location relative to the observer. This formulation emphasizes the disproportionate impact of luminaires closer to the center of the observer's gaze.

Algorithm 1. *SALUSLux intersection simulation.*

Algorithm 1 SALUSLux Intersection Simulation

```
procedure INTERSECTSIMULATION(scenario_params)
    Load IES photometric data for all luminaires
    Initialize grid over all 16 calculation surfaces
    for all grid points (x, y, z) do
        for all light sources L do
            Compute distance d, angles (φ, θ)
            Retrieve I(φ, θ) from interpolated IES data
            Compute E_h
            for all vertical directions N⃗_v do
                Compute E_v
            end for
            E_sc ← Average of E_v
        end for
        Luminance
        GR_any ← Maximum GR from all lights (worst-case)
        GR_dir ← GR in 8 cardinal directions
    end for
    Aggregate results per surface: min, avg, max for each metric
    Log results to CSV and generate visualizations
end procedure
```

The background luminance L_{VE} is modeled as a fraction of the average surrounding luminance, following CIE guidelines:

$$L_{VE} = 0.035 \times L_{\text{average}}$$

Here, L_{average} is the average luminance of the environment, typically calculated within a 1.8m radius around the observation point. This accounts for the eye's adaptation to nearby brightness levels and provides a reference baseline against which glare is perceived.

The GR metric enables SALUSLux to estimate visual discomfort from glare under different lighting scenarios and viewing geometries, providing a critical dimension of safety evaluation in pedestrian lighting analysis.

The GR metric, like many glare-related measures, can often be unintuitive—especially for those new to lighting design. To aid interpretation, we offer a conceptual analogy for future lighting designers: imagine a simplified mental model in which glare is represented by a naive ratio between light falling directly into the eye and the light present in the surrounding environment.

Consider this thought experiment: if someone shines a flashlight directly into your eyes while you're standing in a bright, concrete-paved plaza at midday, the light may be intense, but it won't necessarily feel glaring—because the surrounding environment is well-lit. In this mental model, the "glare ratio" would be small due to the large denominator (ambient luminance). Now imagine the opposite: someone shines the same flashlight in your eyes while you stand in complete darkness. This situation would feel glaring, but in our naive model, it results in a "division by zero" because the denominator—background luminance—is essentially zero. While this simplified analogy breaks down in the extreme, it can serve as a helpful intuition: glare is not just about the brightness of the source, but also about how that brightness contrasts with the visual context around it. The CIE GR formula formalizes this idea by balancing direct veiling luminance against environmental luminance in a logarithmic scale. This perspective is useful for

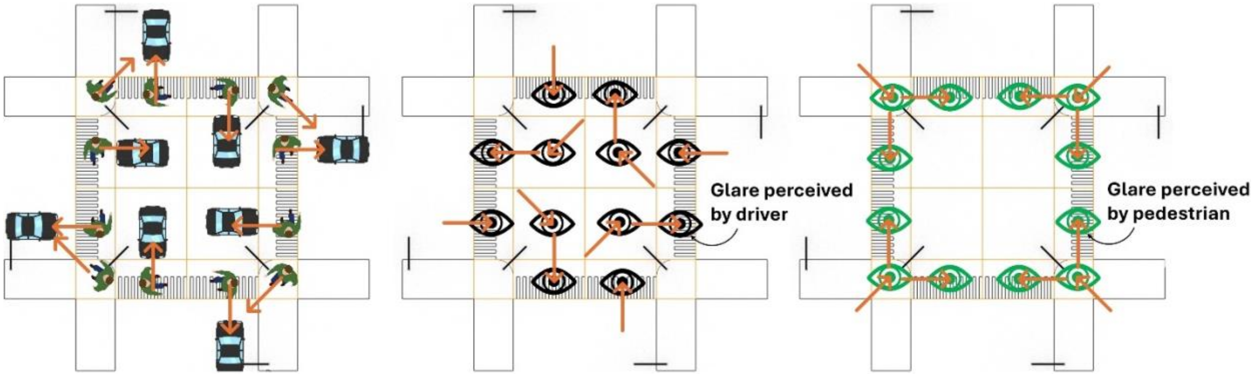

Figure 13. ***Illustration of the set of normal vectors for the calculation of (from left to right): E_v and E_{sc}, GR for drivers, and GR for pedestrians*** **(Kavee at al., 2025).**

developing intuition about why certain lighting configurations—especially those with low ambient luminance—may trigger high GRs, even when using the same luminaires.

3.2.6. Intersection Simulation Setup

A central contribution of this study is the development of the `intersect_simulation` function, which integrates all prior components of the SALUSLux toolkit into a unified workflow for evaluating pedestrian lighting performance. Although the function is demonstrated using a standard four-way intersection as a case study, the underlying simulation framework is fully generalizable and can be adapted to analyze arbitrary roadway geometries and lighting layouts.

The simulation operates by systematically evaluating lighting performance across different configurations and design parameters, computing key metrics including: vertical and semi-cylindrical illuminance (E_v,E_{sc}), luminance (L), and glare rating (GR). These metrics are computed across varying combinations of mounting height, pole offset, orientation, distribution type, color temperature, and wattage. The full process is outlined in Algorithm 1, which captures how each lighting scenario is simulated and assessed.

To evaluate pedestrian visibility, both vertical and semi-cylindrical illuminance are computed with directional vectors aligned to represent realistic observation angles. Specifically, for E_v, the normal vector is oriented along the direction of vehicle travel, simulating how a driver approaching or leaving an intersection would perceive a pedestrian (see Figure 13). For E_{sc}, the simulation includes lateral views to account for turning movements—such as vehicles making left or right turns—which require side-angle visibility of pedestrians.

When computing the GR, observer viewpoints are defined to match typical lines of sight for both pedestrians and drivers. The simulation assumes worst-case glare directions, capturing the most intense luminance observed along likely viewing paths. This ensures that the GR values are both conservative and relevant for design evaluation. These conventions also ensure consistency with the glare heatmaps presented later in the results section, so that the visualizations accurately reflect the modeled observer conditions. By automating the simulation across thousands of scenarios, this framework supports comprehensive evaluation of how intersection lighting design impacts pedestrian safety, visual comfort, and sustainability tradeoffs.

For each simulation scenario, SALUSLux generates a standardized set of visualization outputs, including: horizontal illuminance, vertical illuminance, semi-cylindrical illuminance, glare from any light source (general), glare experienced by drivers, and glare experienced by pedestrians. Examples of these visualizations are shown in Figure 14 and Figure 15.

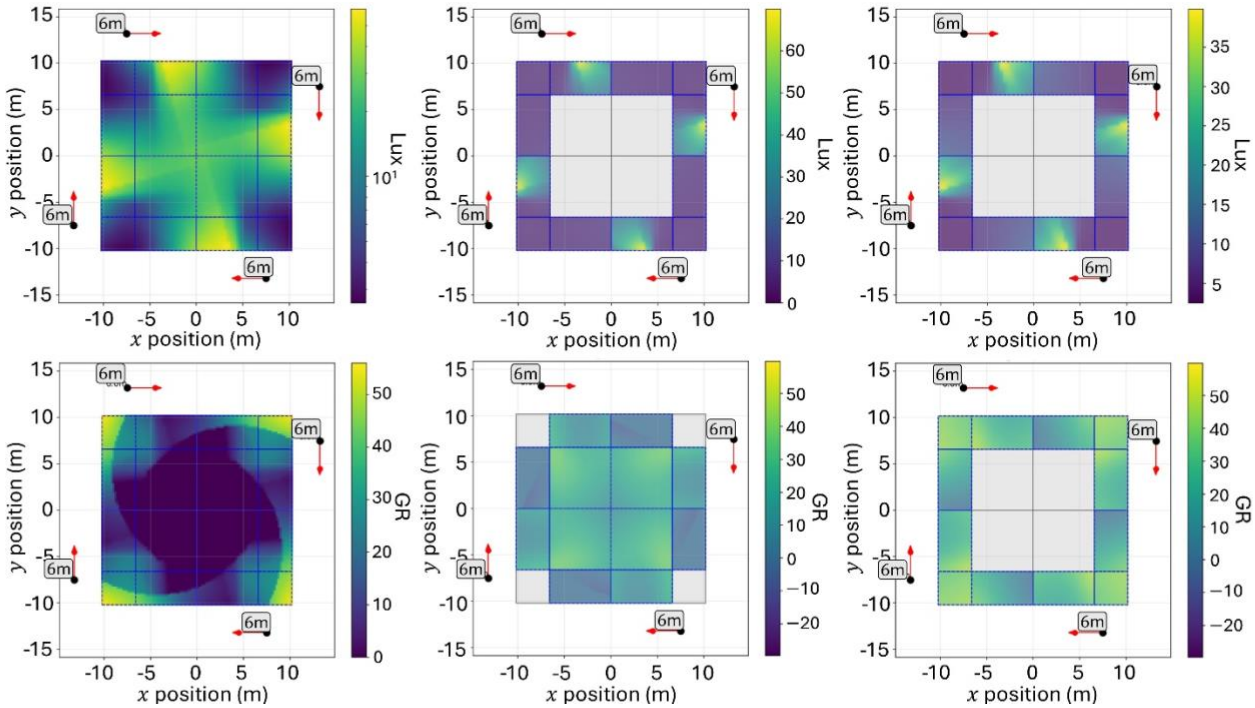

Figure 14. ***Lighting performance of scenario 265, featuring a 90° configuration.***

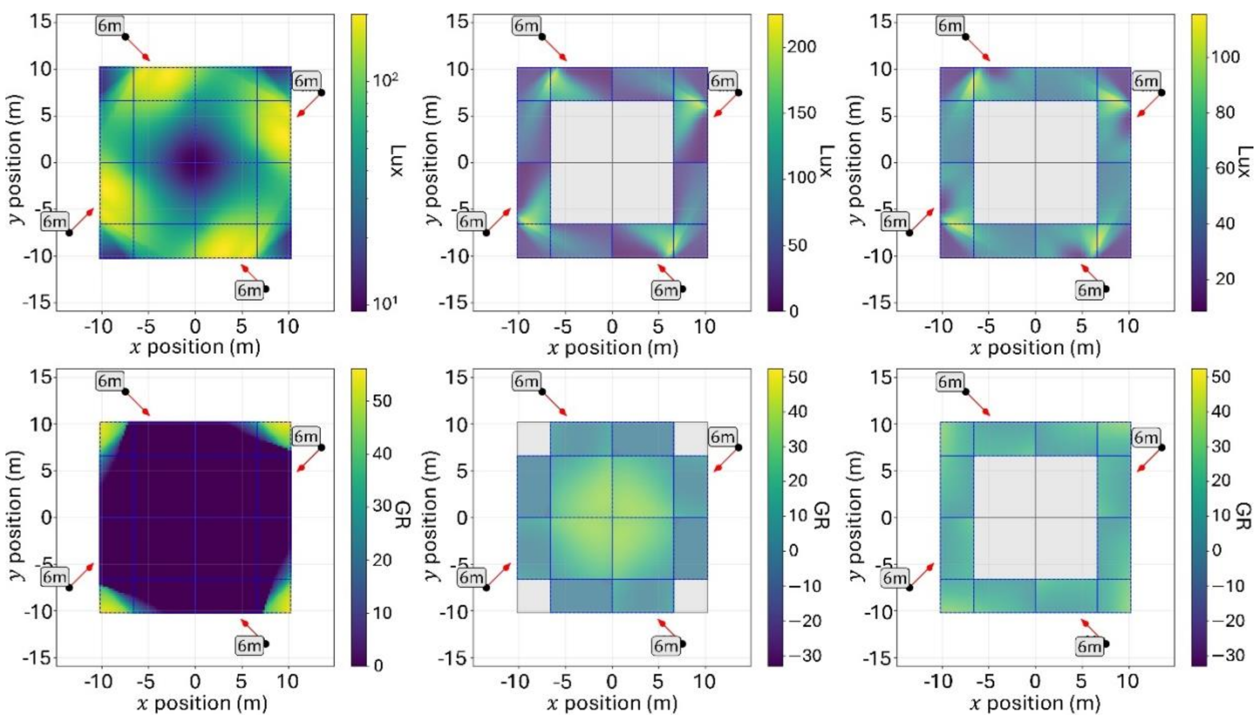

Figure 15. Lighting performance of scenario 414, featuring a 45° configuration.

A deliberate modeling decision was made to visualize general glare values rather than luminance, even though luminance is computed internally. This is because luminance plots tend to resemble horizontal illuminance plots, given that the ground surface reflects most incident light from overhead luminaires in a Lambertian manner. While additional reflective surfaces—such as building walls—could affect luminance in other urban contexts, they are excluded from this study as the modeled environment focuses solely on an open intersection without surrounding structures.

4. Case Study

To demonstrate the capabilities of the SALUSLux software and address the two research questions, we conducted a case study of a four-way intersection, simulating a wide range of lighting design scenarios. The parameters explored in this study fall into two categories: external parameters, which describe the physical layout and placement of the lighting system, and internal parameters, which define the properties of the luminaires themselves. The spatial layout and the designated surface zones for performance evaluation are shown in Figure 8. A total of 2,304 lighting scenarios were generated, combining 32 external configurations with 72 internal configurations.

For the external parameters, we examined two turbine-inspired intersection lighting geometries: a diagonal layout oriented at 45° and a perpendicular layout oriented at 90° relative to the street grid. For each of these layouts, we varied the pole offset ratio—defined as the horizontal distance from the crosswalk corner to the pole, normalized by pole height—at four levels: 0, 0.5, 1.0, and 1.5. These variations capture real-world decisions about how far to place lighting poles from pedestrian zones. Each

Table 5. *Lighting performance thresholds for safety and comfort.*

Metric	Threshold	Motivation
E_h	>24 lux	Based on the intersection road hierarchy, Major/Major requires 18—34 lux and Collector/Collector requires 12—24 lux (Illuminating Engineering Society, 2018).
E_v	>40 lux	30—40 lux vertical average across the center of crosswalk measured at <2m increments (Gibbons et al., 2008; Vanasse Hangen Brustlin, Inc. et al., 2022).
E_{sc}	>40 lux	Crosswalk lighting level of 40 vertical lux (), and a ratio of $E_{sc}/E_v > 1$ is beneficial for facial recognition (Rombauts et al., 1989).
L	>2 cd/m^2	For high pedestrian activity (over 100 PPH) (Vanasse Hangen Brustlin, Inc. et al., 2022).
GR (driver & pedestrian)	>30	Glare is noticeable at $GR = 30$ (CIE, 1994).

Table 6. *Scores awarded to scenarios meeting specified criteria.*

Area	E_h	E_v	E_{sc}	L	GR	GR_{ped}	Sum
NW_m	50	N/A	N/A	50	50	N/A	150
NE_m	50	N/A	N/A	50	50	N/A	150
SW_m	50	N/A	N/A	50	50	N/A	150
SE_m	50	N/A	N/A	50	50	N/A	150
NW	50	50	50	50	N/A	50	250
N_i	50	50	50	50	50	50	300
N_o	50	50	50	50	50	50	300
NE	50	50	50	50	N/A	50	250
E_i	50	50	50	50	50	50	300
E_o	50	50	50	50	50	50	300
SE	50	50	50	50	N/A	50	250
S_i	50	50	50	50	50	50	300
S_o	50	50	50	50	50	50	300
SW	50	50	50	50	N/A	50	250
W_i	50	50	50	50	50	50	300
W_o	50	50	50	50	50	50	300
Sum	800	600	600	800	600	600	4000

Table 7. ***Scenarios with 45° turbine configuration and a GPA of 4.0.***

Scenario	Height	Configuration	Ratio	Temperature	IES type	Wattage	GPA
372	6m	45	1	4,000K	II	151W	4.0
378	6m	45	1	4,000K	III	151W	4.0
384	6m	45	1	4,000K	IV	151W	4.0
390	6m	45	1	3,000K	II	151W	4.0
414	6m	45	1	2,700K	II	151W	4.0

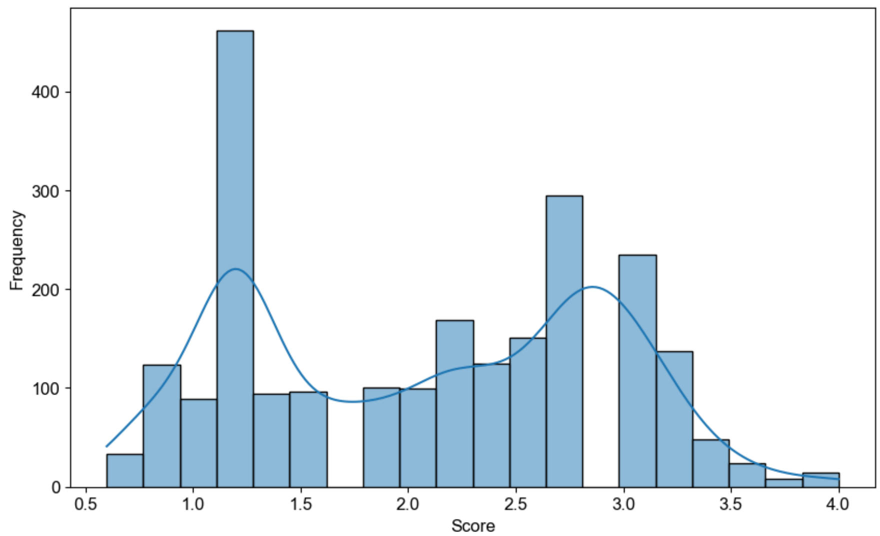

Figure 16. ***Histogram of the main study's GPA distribution with the kernel density estimate overlain.***

configuration was simulated at four different mounting heights: 6.0m, 6.5m, 7.0m, and 7.5m. A fixed horizontal extension from the pole to the luminaire arm was applied across all scenarios.

For the internal parameters, we varied luminaire specifications across two brands and considered four IES distribution types (Type II, III, IV, and V). Each type was tested at three nominal wattages—50W, 100W, and 150W—and three color temperatures: 2,700K, 3,000K, and 4,000K. Although wattages are nominal, the actual power draw varies slightly depending on the manufacturer (e.g., a 100W luminaire may draw 104.5W). These internal specifications were cross-combined with each external layout to ensure a comprehensive exploration of performance across lighting technologies and geometries.

For each of the 2,304 scenarios, SALUSLux exported: (1) CSV logs of minimum, average, and maximum values for each metric per surface; (2) six heatmaps per scenario (E_h, E_v, E_{sc}, GR (any angle), GR, GR_{ped}; and (3) a scenario score based on whether the metric thresholds were met, as listed in Table 5.

4.1. Scoring Framework

To enable performance comparisons across the 2,304 lighting scenarios, we developed a scoring framework based on metric-specific thresholds (defined in Table 5). Each scenario earns 50 points for every surface where a lighting metric meets or exceeds its performance threshold (Table 6). However, certain surface-metric combinations are considered inapplicable. For example, the four middle sidewalk zones (NW_m, NE_m, SW_m, SE_m) are not directly associated with pedestrian crossings, making vertical and semi-cylindrical illuminance measurements irrelevant. These exclusions are summarized in Table 6.

After excluding inapplicable combinations, each scenario is evaluated across 80 valid metric-surface pairs, resulting in a maximum achievable score of 4,000 points. We normalize this score to a 4.0 scale, which we

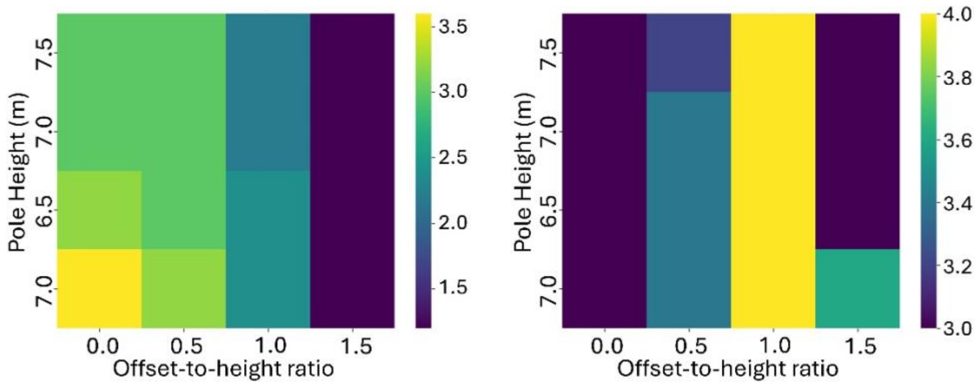

Figure 17. ***A heatmap of scores (GPA out of 4.0) for external variation analysis for 90° turbine configuration (left) and 45° turbine configuration (right). The vertical axis is pole height and horizontal axis is the offset-to-z ratio.***

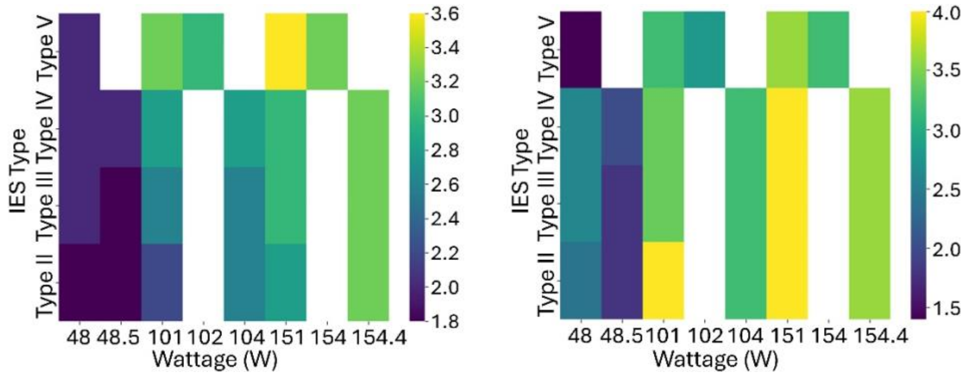

Figure 18. ***A heatmap of scores (GPA out of 4.0) for internal variation analysis for 90° turbine configuration (left) and 45° turbine configuration (right). The vertical axis is IES Type and horizontal axis is the wattage.***

refer to as the GPA. A perfect score of 4.0 indicates that the lighting design met or exceeded the threshold in every applicable metric-surface pair. While the default implementation assigns equal weight to all metrics, the framework is customizable. Users may adjust scoring priorities to align with specific objectives—such as emphasizing pedestrian safety, minimizing light pollution, or balancing both. For this case study, equal weighting is applied across all metrics to explore general performance trends.

5. Results

This section presents the performance results of 2,304 intersection lighting scenarios simulated using the SALUSLux toolkit. Each scenario combined different lighting geometries—including pole placement, height, and offset—with varying luminaire characteristics such as distribution type, wattage, and CCT. The distribution of overall scores, normalized to a 4.0 GPA scale, is shown in Figure 16.

5.1. Main Study

We first examined how variations in external parameters affected lighting performance. For both the 90° and 45° turbine configurations, we identified the highest-scoring scenarios and compared how performance changed across different pole heights and offset ratios. Interestingly, in the 90° configuration, increasing pole height resulted in a consistent decline in overall performance. This may reflect how higher poles reduce near-field illuminance and increase the potential for glare. In contrast, pole height had little

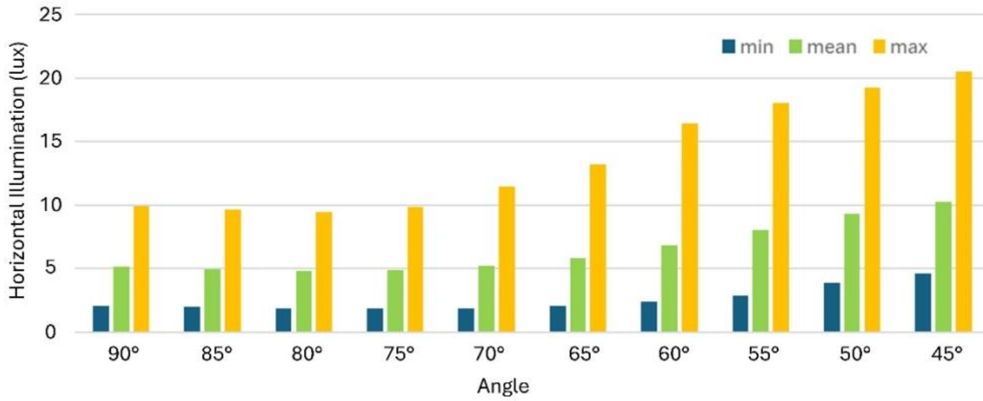

Figure 19. ***Horizontal illumination on the adjacent land of the right of way for each turning angle.***

effect on performance in the 45° configuration, which may better distribute light across the intersection regardless of mounting height. Similarly, larger horizontal offsets (i.e., poles placed farther from the intersection corner) generally degraded performance in the 90° setup but had minimal impact in the 45° configuration. These relationships are illustrated in Figure 17 and Figure 18.

Top-performing scenarios in the 90° configuration featured a Type V IES distribution paired with an LED luminaire consuming approximately 151W. These scenarios consistently achieved high scores despite some of the geometric drawbacks of the 90° layout. In contrast, the 45° layout reached perfect GPA scores using a range of distribution types—Type II, III, and IV—when combined with the same wattage. The Type II distribution, in particular, stood out for its efficiency: it delivered a perfect 4.0 GPA with a slightly lower power consumption of around 101W.

Notably, a 2,700K color temperature—aligned with DarkSky best practices for reducing light pollution—also achieved a perfect score when paired with a Type II distribution and 150W power level. This configuration represents an ideal balance between minimizing environmental impact and ensuring pedestrian safety. The spatial performance of this scenario is visualized in Figure 15, where clear lighting coverage and controlled glare reflect the benefits of this design combination.

Summary of key findings:

The simulations revealed strong interaction effects between spatial geometry (external) and luminaire properties (internal).

External Variation

1. 90° Turbine configurations were more sensitive to pole height and offset than 45° turbine configurations (Figure 17).
2. 45° turbine configurations consistently achieve higher scores across wattage and CCT variations, particularly at lower pole heights (6.0m) and moderate offsets (1.0× pole height). Intuitively, this configuration better illuminated multiple pedestrian-facing angles and covered the other side of outgoing traffic.

Internal Variation

1. The IES Type II distribution offered the best balance across both configurations, especially when paired with a 151W LED luminaire.
2. For 45° turbine configuration, an LED luminaire with a power of 151.0W still comes on top, but now also with IES distribution Type II, Type III, and Type IV (see Table 7). Interestingly, Type II distribution

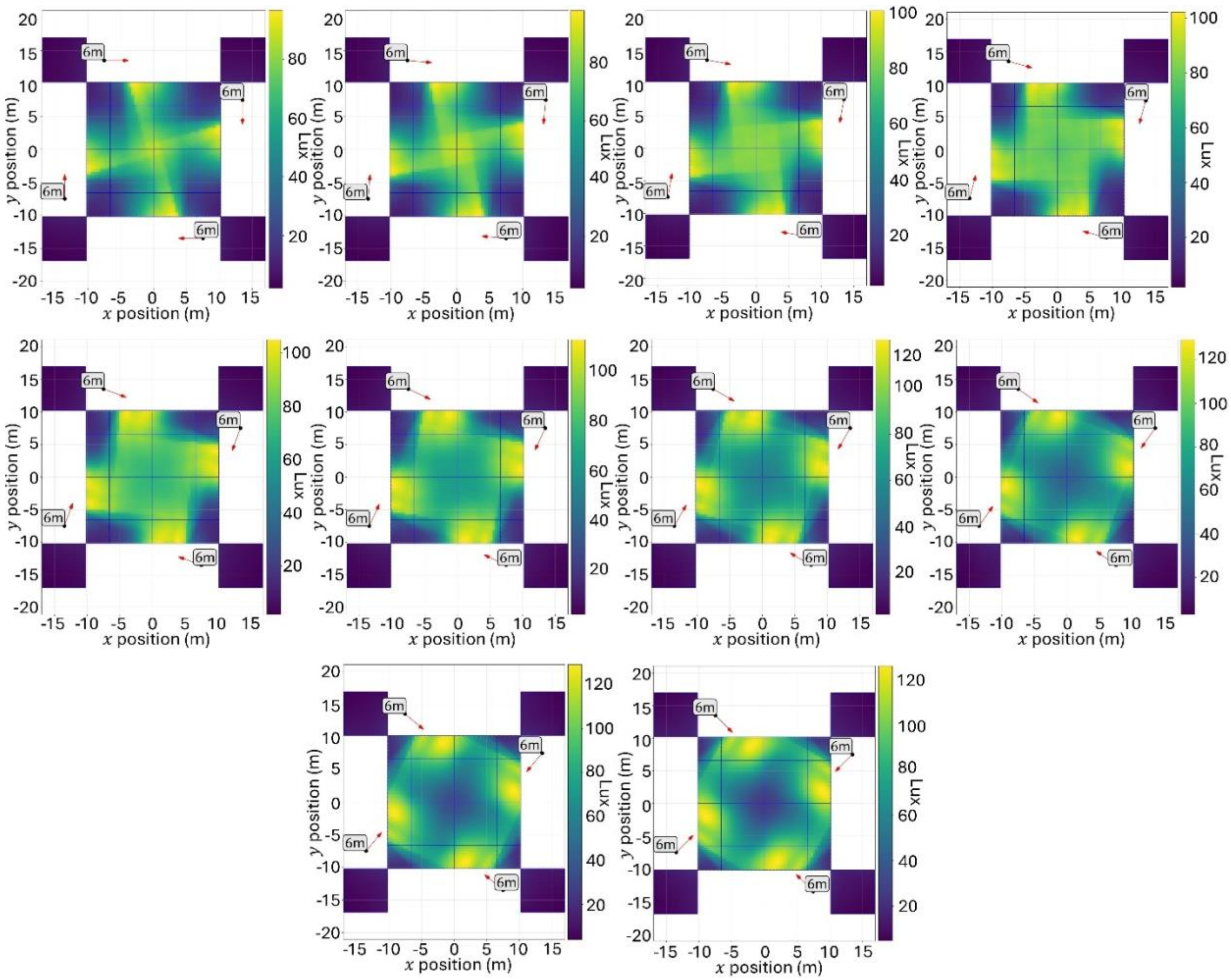

Figure 20. ***Heatmaps of horizontal illuminance with four adjacent areas to assess light trespass. From left to right: (Top) 90°, 85°, 80°, 75°; (Middle) 70°, 65°, 60°, 55°; (Bottom) 50°, 45°.***

appears to be a good choice for 151.0 and 101.0W. If we focus on the color temperature, a streetlight with 2700K can still achieve a GPA of 4.0 by using IES Distribution Type II at about 150W. This design is by far the most preferred design for DarkSky concerns, as seen in Figure 19.

5.2. Angle Search for Light Trespassing

When a luminaire is oriented at an angle less than 90° relative to the roadway, its beam may extend beyond the public right-of-way and intrude onto adjacent private property. To investigate this potential for light trespass, we modified the previous scenario by adjusting the pole orientation in 5° increments between 45° and 90°. All other parameters were held constant, consistent with Scenario 414, for simplicity:

- Pole height: 6m
- Horizontal offset: 6m (1.0 × height)
- Luminaire: Cooper "ARCH-M-PA2-150-727-U-T2R.ies" IES file

The analysis focused on horizontal illuminance in the adjacent area on the northeast side of the intersection (which is symmetrical to the other three sides). Results for the ten angle configurations are

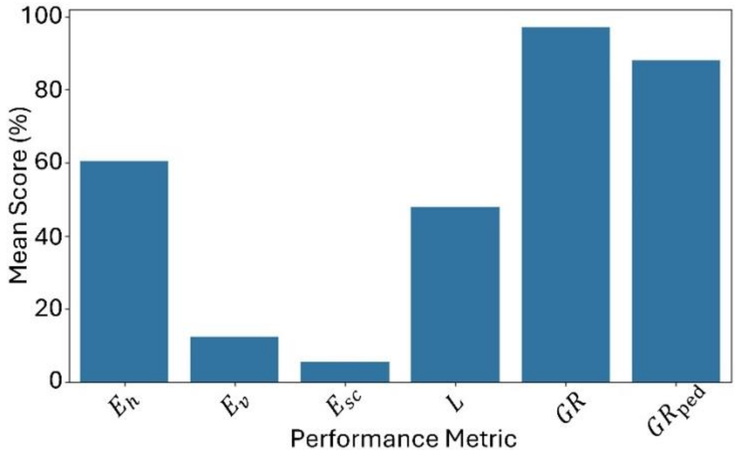

Figure 21. ***Comparison among performance metrics. Low mean score implies a higher level of achievement difficulty.***

shown in Figure 19. As expected, light trespass increased as the orientation shifted from 90° to 45°. Interestingly, a small local minimum was observed at 80°. Ignoring this small dip, the data show that light trespass remains around 5 lux on average for orientations no lower than 70°, and increases to approximately 10 lux when the orientation is reduced to 45°. This gradual transition is illustrated in Figure 20.

6. Discussion

By simulating more than 2,000 multidirectional lighting configurations, this study highlights the critical role of interactions between light source properties and spatial layout in determining real-world performance. This section discusses key implications for practice and policy, as well as potential directions for future research.

6.1. Combined Effects of Light Source and Geometry

The simulations demonstrated pronounced interaction effects between spatial geometry and luminaire properties. The 90° turbine configurations were notably more sensitive to both pole height and offset distance than the 45° configurations. As pole height increased or as the offset exceeded 1.0×, both vertical and semi-cylindrical illuminance levels declined, reducing pedestrian visibility. In contrast, the 45° layout provided more consistent lighting performance, particularly in illuminating multiple pedestrian-facing angles, including those encountered by turning vehicles.

Among the performance metrics, semi-cylindrical illuminance emerged as the most challenging criterion to satisfy across all scenarios, as shown in Figure 21. Unlike vertical illuminance, which measures light on a single plane, semi-cylindrical illuminance better represents the three-dimensional visibility of pedestrians—a critical factor at corners where right-turning vehicles approach from side angles. The results of this study reinforce growing evidence that semi-cylindrical illuminance should be prioritized as a required standard for intersection crosswalk lighting.

Furthermore, the findings suggest that horizontal illuminance should be de-emphasized as a primary design metric. While horizontal illuminance contributes indirectly to other measures such as luminance and glare, it does not provide additional benefits once these metrics meet their thresholds. Overemphasis on horizontal illuminance could even encourage excessive lighting, inadvertently increasing light pollution without improving pedestrian safety. Therefore, lighting design practices should focus on metrics directly tied to visibility and comfort rather than defaulting to horizontal illuminance as a performance target.

6.2. Design Implications and Spatial Constraints

Although Scenario 414—and other top-performing configurations listed in Table 7—met all simulated performance benchmarks, several practical constraints must be considered for real-world deployment. Turbine-style layouts, particularly those incorporating pole offsets, are highly effective at illuminating pedestrians approaching from the incoming traffic direction. However, these configurations can also push light beyond the boundaries of the right-of-way, potentially spilling onto private property or adjacent buildings. For instance, in the 45° turbine configuration with a Type II luminaire, some of the light distribution extended past the designated evaluation zones and onto nearby facades.

A critical but often overlooked component of pedestrian safety is visual contrast—the degree to which a pedestrian stands out against the background, particularly from the driver's viewpoint. Positive contrast occurs when the pedestrian appears brighter than their surroundings, enhancing visibility and reaction time. In Scenario 414, the crosswalk area at location W_i receives vertical illuminance (E_v) of 75.90 lux and semi-cylindrical illuminance (E_{sc}) of 59.88 lux, both significantly higher than the horizontal illuminance ($E_h = 48.71$ lux) of the nearby asphalt at location SW_m. Assuming a skin reflectance factor of 0.4, the estimated luminance of a pedestrian at W_i is 9.66 cd/m², compared to 3.10 cd/m² for the asphalt. This results in an absolute contrast of 6.56 cd/m² and a luminance ratio of 3.11, indicating strong positive contrast that supports effective pedestrian detection under nighttime conditions.

6.3. A Feasible Balance of Performance and Light Pollution Tradeoffs

Contrary to the common assumption that enhancing pedestrian visibility requires high-intensity or high-CCT lighting, this study found that environmentally sensitive lighting designs—such as 2,700K LED luminaires—can still meet or exceed performance thresholds for visibility and glare control. This challenges the perceived tradeoff between pedestrian safety and sustainability, demonstrating that both can be achieved simultaneously.

The highest-performing configuration in the simulation featured:

- A 2,700K, 151W LED luminaire,
- Type II distribution,
- A 6.0m pole height, and

A 1.0× offset in the 45° turbine configuration.

This setup aligned with DarkSky International recommendations for reducing light pollution while still delivering strong performance across vertical illuminance, semi-cylindrical illuminance, and glare metrics. In short, "dark sky-friendly" streetlighting does not inherently compromise safety at intersections.

However, it is important to note that these findings apply specifically to intersections, not continuous roadway segments. A 6m pole may be too short for extended road segments, potentially leading to uneven lighting distribution unless additional luminaires are installed. As such, we recommend that intersection lighting design criteria be considered separately from roadway lighting criteria, allowing cities to adopt context-specific solutions that balance safety and environmental responsibility.

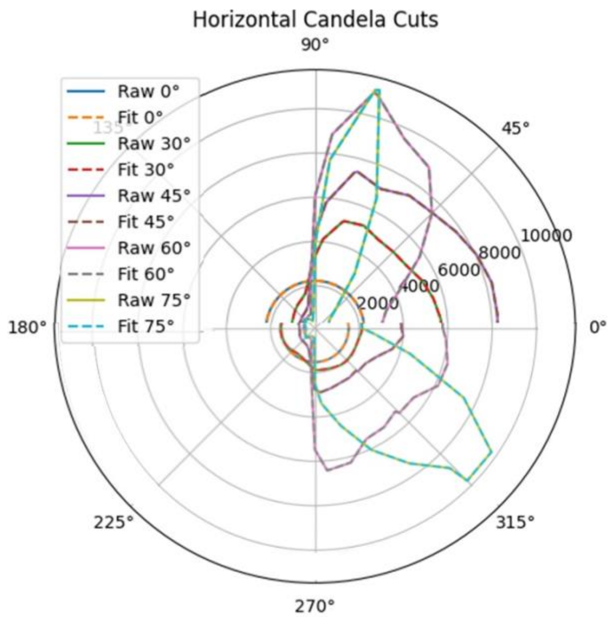

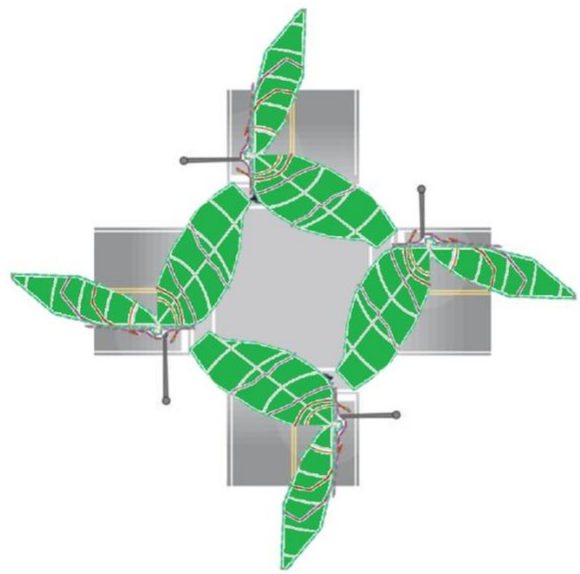

Figure 22. ***A representative fusion of IES Type II and Type IV distributions for street lighting.***

7. Recommendations

This study demonstrates that pedestrian-centered intersection lighting can be achieved without compromising environmental sensitivity or exceeding common design constraints. Based on our findings, we propose the following four key recommendations for future research, practice, and standards development:

1. Account for Reflectance and Real-World Variability: SALUSLux simulations assumed uniform reflectance values (e.g., ρ = 0.2 for asphalt), but real-world variation in materials (e.g., wet pavement, concrete, or textured surfaces), weather, and clothing can significantly affect luminance and visibility. Future simulations and design tools should incorporate dynamic surface and environmental parameters to reflect more realistic operating conditions.
2. Improve Modeling of Glare Perception: The current GR calculations are based on the standardized CIE formula. However, actual glare perception varies based on age, eye adaptation, and the presence of other competing visual stimuli in the environment. Expanding the SALUSLux framework to include empirical models of subjective glare perception—or to incorporate user-specific profiles—would improve its applicability in practice.
3. Expand Light Trespass Modeling Beyond Right-of-Way: Our analysis was limited to 16 interior and edge surfaces within the right-of-way. Light trespass into adjacent private properties, building façades, or vegetation was not assessed. For cities committed to minimizing environmental and ecological light pollution, we recommend future simulation tools include spatial domains beyond the right-of-way to quantify and mitigate unintended light spillover.
4. Introduce a New "Intersection-Type" IES Distribution: The simulations revealed that current IES distribution types are not optimized for intersection lighting. Often, only half of the luminaire's beam is functionally used for illuminating crosswalks; the remaining beam pattern is oriented along street segments. To address this inefficiency, we propose the development of a new IES "intersection-type" distribution—Type VII—which integrates the strengths of existing Type II and either Type I, III, or IV distribution depending on roadway configuration.

Specifically, this proposed distribution uses a Type II pattern for the 0°–180° horizontal range, which faces the intersection and pedestrian activity, and a Type IV pattern for the 180°–360° range, oriented toward approaching drivers along the street segment. This hybrid distribution, shown in Figure 22, would better target light to areas of highest need while minimizing unnecessary spill and energy use. Our simulations indicate this pattern could support high-performance, low-glare intersection lighting while preserving dark-sky principles.

8. Conclusions

This study shows that designing effective intersection lighting requires a multidimensional approach—one that integrates spatial geometry, human visibility metrics, and environmental considerations alongside luminaire selection.

Using the custom-built, open-source SALUSLux simulation toolkit, we evaluated 2,304 lighting configurations across a standard four-leg intersection. These scenarios varied both in physical layout and photometric properties. The results demonstrate that intersections demand lighting strategies distinct from those used for road segments. Specifically, successful designs must illuminate pedestrians from multiple angles, minimize glare, and support sustainability goals. Two major insights emerged:

1. Joint optimization of geometry and light source properties leads to superior safety outcomes. Rather than treating layout and lighting independently, their combined effects should be considered. For example, a turbine-style configuration at 45°, paired with a 2700K, Type II, 150W LED at 6m and 1.0× offset, achieved perfect scores across all pedestrian visibility metrics.
2. Safe lighting does not require high-CCT or high-wattage luminaires. With thoughtful spatial placement, aiming direction, and beam control, designers can meet or exceed safety thresholds while avoiding unnecessary brightness and mitigating light pollution.

SALUSLux provides a replicable, programmable framework for evaluating intersection-specific lighting performance. It enables rapid exploration of design alternatives that would be difficult or time-consuming with conventional tools, and it supports future integration with sensor networks, adaptive control systems, and climate-responsive infrastructure.

In short, a better-lit future for pedestrians does not mean simply making everything brighter. Rather, it means being brighter where it matters, darker where it doesn't—and smarter everywhere in between.

9. Appendix

1. For more information and contribution to SALUSLux, see the online repository at GitHub: https://github.com/CMU-SALUS-Lab/saluslux.
2. At the time of this study, DIALux evo, available at https://www.dialux.com/en-GB/dialux (free), does not allow a direct import of IES files.

10. Acknowledgements

This work was supported in part by the U.S. Department of Transportation University Transportation Center Safety21 and the Ministry of Higher Education, Science, Research and Innovation in Thailand (MHESI) of the Royal Thai Government [Unit 0330084: Smart Civil Engineering].

11. References

American Association of State Highway and Transportation Officials (AASHTO). (2018). *Roadway lighting design guide* (7th ed.). https://trid.trb.org/View/1565773

Baker, M. (2025). The LED debacle: Chapter 1—Why is LED light different? https://www.softlights.org/why-is-led-light-different/

CIE. (1994). Glare evaluation system for use within outdoor sports and area lighting (Publication No. 112).

DarkSky International. (2025). DarkSky International | Protecting the night skies for present and future generations. https://darksky.org/

Edwards, C. J., & Gibbons, R. B. (2008). Relationship of vertical illuminance to pedestrian visibility in crosswalks. Transportation Research Record: Journal of the Transportation Research Board, 2056(1), 9–16. https://doi.org/10.3141/2056-02

Elvik, R. (1995). Meta-analysis of evaluations of public lighting as accident countermeasure. Transportation Research Record, 1485(1), 12–24.

Falchi, F., Cinzano, P., Duriscoe, D., Kyba, C. C., Elvidge, C. D., Baugh, K., Portnov, B. A., Rybnikova, N. A., & Furgoni, R. (2016). The new world atlas of artificial night sky brightness. Science Advances, 2(6), e1600377. https://doi.org/10.1126/sciadv.1600377

Fotios, S., & Gibbons, R. (2018). Road lighting research for drivers and pedestrians: The basis of luminance and illuminance recommendations. Lighting Research & Technology, 50(1), 154–186. https://doi.org/10.1177/1477153517739055

Gibbons, R., Edwards, C., Williams, B. M., & Andersen, C. (2008, April 1). Informational report on lighting design for midblock crosswalks. https://www.semanticscholar.org/paper/Informational-Report-on-Lighting-Design-for-Gibbons-Edwards/6ffca57ae49389234ea12a5a6704402bff772967

Governors Highway Safety Association. (2024). Pedestrian traffic fatalities by state: 2023 preliminary data (January–December). https://www.ghsa.org/resources/Pedestrian-Traffic-Fatalities-by-State-2023-Preliminary-Data

Highways Industry. (2015). How to prevent streetlight glare in the new world of LED lighting. https://www.highwaysindustry.com/how-to-prevent-streetlight-glare-in-the-new-world-of-led-lighting/

Hu, W., Houten, R. V., Cicchino, J. B., Engle, J., & Shomaly, L. A. (2025). Effects of crosswalk illuminators and rectangular rapid flashing beacons on speed reductions and yielding to pedestrians at night. Transportation Research Record: Journal of the Transportation Research Board. https://doi.org/10.1177/03611981241310131

Illuminating Engineering Society (IES). (2018). American national standard practice for design and maintenance of roadway and parking facility lighting. Illuminating Engineering Society.

Illuminating Engineering Society (IES). (2019). Approved method: IES standard file format for the electronic transfer of photometric data and related information (No. ANSI/IES LM-63-19). Illuminating Engineering Society. https://store.ies.org/product/lm-63-19-approved-method-ies-standard-file-format-for-the-electronic-transfer-of-photometric-data-and-related-information/

Kavee, K., Flanigan, K.A., & Quick, S. (2025). SALUSLux: Open-source street lighting software to improve pedestrian safety and light pollution. Proceedings of the 11th IEEE International Smart Cities Conference, Patras, Greece, October 06-09, IEEE, 2025.

Khodasevich, D., Tsui, S., Keung, D., Skene, D., & Martinez, M. E. (2020). The influence of light pollution and light-at-night on the circadian clock. medRxiv: The Preprint Server for Health Sciences.

Kidd, D. G., & Spivey, W. (2024). A case study of nighttime pedestrian automatic emergency braking performance under different roadway lighting and pedestrian clothing conditions. Traffic Injury Prevention, 25, S250–S253.

Li, Y., Bhagavathula, R., Terry, T., Gibbons, R., & Medina, A. (2020). Safety benefits and best practices for intersection lighting (Nos. VTRC20-R3). Virginia Tech Transportation Institute. https://vtrc.virginia.gov/media/vtrc/vtrc-pdf/vtrc-pdf/20-R31.pdf

Link, M. (2024). Pedestrian deaths spike right after sunset. https://ssti.us/2024/03/25/pedestrian-deaths-spike-right-after-sunset/

MacEvoy, B. (2025). Color making attributes. https://www.handprint.com/HP/WCL/color1.html

Miller, N. (2019, July 17). The elusive discomfort glare metric. https://www.ies.org/fires/the-elusive-discomfort-glare-metric/

National Academies of Sciences & Medicine. (2011). Women's issues in transportation: Summary of the 4th international conference, Volume 1: Conference overview and plenary papers. https://nap.nationalacademies.org/catalog/22901/womens-issues-in-transportation-summary-of-the-4th-international-conference-volume-1-conference-overview-and-plenary-papers

Ossila. (2025). What is luminance? https://www.ossila.com/pages/what-is-luminance

Painter, K. (1996). The influence of street lighting improvements on crime, fear and pedestrian street use, after dark. Landscape and Urban Planning, 35(2), 193–201. https://doi.org/10.1016/0169-2046(96)00311-8

Remaking Cities Institute. (2016). LED street light research project – part II: New findings. Carnegie Mellon University. https://www.cmu.edu/metro21/projects/net-zero-energy/led-street-lights.html

Rombauts, P., Vandewyngaerde, H., & Maggetto, G. (1989). Minimum semicylindrical illuminance and modelling in residential area lighting. Lighting Research & Technology, 21(2), 49–55. https://doi.org/10.1177/096032718902100201

Singh, P. P., & Garg, R. D. (2013). Study of spectral reflectance characteristics of asphalt road surface using geomatics techniques. 2013 International Conference on Advances in Computing, Communications and Informatics (ICACCI), 516–520. https://doi.org/10.1109/ICACCI.2013.6637225

Smart Growth America. (2025). Dangerous by design 2024: An urgent call to prioritize pedestrian safety. https://smartgrowthamerica.org/dangerous-by-design-2024/

Sullivan, J. M., & Flannagan, M. J. (1999). Assessing the potential benefit of adaptive headlighting using crash databases. University of Michigan, Ann Arbor, Transportation Research Institute.

Terry, T., Gibbons, R., Kassing, A., Bhagavathula, R., Lowdermilk, C., & Lutkevich, P. (2020). Research report: Street lighting for pedestrian safety. Virginia Tech Transportation Institute. https://safety.fhwa.dot.gov/roadway_dept/night_visib/docs/StreetLightingPedestrianSafety.pdf

Transportation Association of Canada (TAC). (2006). Guide for the design of roadway lighting (Publication code PTM-LIGHTING06-E). Ottawa, Ontario, Canada. https://www.tac-atc.ca/en/knowledge-centre/technical-resources-search/publications/ptm-lighting06-e/

Transportation Research Board (TRB). (1974). Warrants for highway lighting: NCHRP Report 152. Washington, DC: Transportation Research Board. https://onlinepubs.trb.org/Onlinepubs/nchrp/nchrp_rpt_152.pdf

Vanasse Hangen Brustlin, Inc., Virginia Tech Transportation Institute, & FHWA Office of Safety. (2022). Pedestrian lighting primer (FHWA-SA-21-087).

Virtanen, P., Gommers, R., Oliphant, T. E., Haberland, M., Reddy, T., Cournapeau, D., Burovski, E., Peterson, P., Weckesser, W., & Bright, J. (2020). SciPy 1.0: Fundamental algorithms for scientific computing in Python. Nature Methods, 17(3), 261–272.

Wood, J. M. (2020). Nighttime driving: Visual, lighting and visibility challenges. Ophthalmic and Physiological Optics, 40(2), 187–201. https://doi.org/10.1111/opo.12659

Younes, H., Noland, R. B., Von Hagen, L. A., & Meehan, S. (2023). Pedestrian- and bicyclist-involved crashes: Associations with spatial factors, pedestrian infrastructure, and equity impacts. Journal of Safety Research, 86, 137–147. https://doi.org/10.1016/j.jsr.2023.05.005